BEYOND THE STANDARD MODEL

By

BHASKAR DUTTA

Bachelor of Science
Presidency College
University of Calcutta, Calcutta, India
1987

Master of Science
University of Calcutta
Calcutta, India
1990

Submitted to the Faculty of the
Graduate College of the
Oklahoma State University
in partial fulfillment of
the requirements for
the Degree of
DOCTOR OF PHILOSOPHY
July, 1995

OKLAHOMA STATE UNIVERSITY

BEYOND THE STANDARD MODEL

Thesis Approved:

Satyanarayan Nandi
Thesis Adviser

Mark Samuel (LV)

Thomas C. Collins
Dean of the Graduate College

ACKNOWLEDGMENTS

First and foremost, I wish to extend my thanks to my advisor Dr. Satyanarayan Nandi without whose sincere help my PhD work would not have reached its completion. He was involved at every stage of this work. I am grateful to him for going through the manuscript in meticulous details.

Many other individuals have also helped me throughout my research. In particular, I would like to acknowledge Dr. Duane Dicus, Dr. Tatsu Takeuchi, Dr. Evan Keith, Dr. Scott Willenbrock for their sustained adherence. My thanks are also due to Dr. Mark Samuel, Dr. Larry Scott and Dr. Birne Binegar for being present in my PhD Advisory Committee and providing me with all the support that I needed. I wish to thank my office-mates Mr. Tesfaye Abraha, Mr. Steve Gibbons, Mr. Appollo Mian, Mr. Eric Steifeld, Mr. Steve Narf, Mr. Dave Muller for keeping my spirit high during my hard-working days. I like to thank espesially Mr. Abraha for pointing out some serious typing errors.

I am indebted to my parents Mrs. Jharna Dutta and Mr. Shyamal Kr. Dutta for their neverending support and encouragement while I got spoiled in physics. Finally, I thank my wife Nandita for putting up with me while I was writing, for being there when I needed her, for reading the proof, and for keeping me from going crazy.

TABLE OF CONTENTS

LIST OF TABLES

LIST OF FIGURES

CHAPTER I

INTRODUCTION

The Standard Model

The Standard Model[1] seems to be consistent with the known experimental results. It is non-abelian gauge theory[2] based on the gauge group $SU(3)_c \times SU(2)_L \times U(1)_Y$. Let me describe some basic features of the Standard Model.

Every gauge theory possesses one massless spin-1 field for each generator of the gauge group. For Standard model, $SU(3)_c$ is unbroken. It has eight massless generators called gluons. The remaining groups $SU(2)_L \times U(1)_Y$ get spontaneously broken down to $U(1)_{em}$ producing 3 massive gauge bosons $W^{\pm}$ and Z . Since $U(1)_{em}$ is left over, we have a massless gauge boson called photon.

In addition to the gauge bosons which are the minimal particle content of any gauge theory, the most general renormalizable theory[3] may contain spin-0 and spin-1/2 fields. The Lagrangian based on the most general gauge theory $SU(3)_c \times SU(2)_L \times U(1)_Y$ may be written as

$$L = L_k + L_s + L_f + L_Y \tag{1}$$

where L_k contains the gauge boson kinetic terms, L_f contains the fermions kinetic term, $L_s$contains the scalars mass terms, kinetic energy terms, as well as self interactions, and L_Y ,the Yukawa sector , contains interaction between the fermions and the scalars. Explicitly, the terms in the eqn.(1) are

$$L_k = -\frac{1}{4}B^{\mu\nu}B_{\mu\nu} - \frac{1}{4}W_{\mathrm{i}}^{\mu\nu}W_{\mu\nu,\mathrm{i}} - \frac{1}{4}G_{\mathrm{i}}^{\mu\nu}G_{\mu\nu,\mathrm{i}}, \tag{2}$$

$$L_s = (D^{\mu}\Phi)^{\dagger}(D_{\mu}\Phi) - V(\Phi), \tag{3}$$

$$L_f = \overline{\Psi}(\mathrm{i}D)\Psi, \tag{4}$$

$$L_Y = H(\Psi, \overline{\Psi}, \Phi), \tag{5}$$

where the quantities $B^{\mu\nu}, W_{\mathrm{i}}^{\mu\nu}, G_{\mathrm{i}}^{\mu\nu}$ are the gauge bosons' field strength tensors and, D^{μ}, the covariant derivative, is given by

$$D^{\mu} = \partial_{\mu} + \mathrm{i}g_s I_{\mathrm{i}} G_{\mathrm{i}}^{\mu} + \mathrm{i}g_s T_{\mathrm{i}} W_{\mathrm{i}}^{\mu} + \mathrm{i}g\frac{Y}{2}B_{\mathrm{i}}^{\mu} \tag{6}$$

The constants g_s, g, and g are , the coupling constants of $SU(3), SU(2)$,and $U(1)$ respectively. $I_{\mathrm{i}}, T_{\mathrm{i}}, \frac{Y}{2}$ are the representations for the gauge group's generators. $V(\Phi)$contains all scalar interactions of quartic and lower order and $H(\Psi, \overline{\Psi}, \Phi)$ contains all interactions that are linear in $\Psi, \overline{\Psi}$ and Φ. The Ψs represent the fermions. Standard Model has two kinds of fermions: quarks and leptons. Between them, there are 15 fermions divided into 3 generations:

Ist generation: $\begin{pmatrix} u \\ d \end{pmatrix}_L, u_{R,}, d_{R,} \begin{pmatrix} \nu_e \\ e \end{pmatrix}_L, e_{R.}$where u, d are up and down quarks, ν_e, e are electron neutrino and electron. L and R stand for the helicities. So, the left-handed particles are in $SU(2)$ doublet and the right-handed particles are the $SU(2)$ singlets.

2nd generation : $\begin{pmatrix} c \\ s \end{pmatrix}_L, c_{R,}, s_{R,} \begin{pmatrix} \nu_\mu \\ \mu \end{pmatrix}_L, \mu_{R.}$where c, s are charm and strange quarks, ν_μ, μ are muon neutrino and muon. L and R stand for the helicities.

2nd generation : $\begin{pmatrix} t \\ b \end{pmatrix}_L, c_{R,}, s_{R,} \begin{pmatrix} \nu_\tau \\ \tau \end{pmatrix}_L, \tau_{R.}$where t, b are top and bottom quarks, ν_τ, τ are muon neutrino and taon.

In the minimal model, we can assume one scalar doublet :

$$\Phi = \begin{pmatrix} \Phi^+ \\ \Phi^0 \end{pmatrix}, \tag{7}$$

Given these particle assignments, it is possible to write down the most general V and H that appear in Eqn.(4),(5).

$$L_s = (D^{\mu}\Phi)^{\dagger}(D_{\mu}\Phi) + \mu^2\Phi^{\dagger}\Phi - \frac{1}{2}\lambda\left(\Phi^{\dagger}\Phi\right)^2, \text{and} \tag{8}$$

$$L_Y = -h_e\overline{e_R}\Phi^{\dagger}L_L - h_d\overline{d_R}\Phi^{\dagger}Q_L - -h_u\overline{u}_R\Phi_c^{\dagger}Q_L + \text{h.c.} \tag{9}$$

where μ is a constant with dimension of a mass, and λ, h_e,h_d and h_u are dimensionless constants. The field Φ_c is the charge conjugate of Φ, defined as

$$\Phi_c = \mathrm{i}\sigma_2\Phi^*, \tag{10}$$

where σ_2 is one of the Pauli matrices.

So far, we have not yet talked about the masses of these bosons and fermions. Since we live in a real world, we need to have masses for them and they get generated through spontaneous symmetry breaking[4]. That is to say, though the lagrangian is invariant under $SU(3)_c \times SU(2)_L \times U(1)_Y$,the ground state is not invariant. The scalar potential in (8)is minimized for $\mid \Phi \mid^2 = v^2$,with $\mathrm{v}^2 \equiv \frac{\mu^2}{\lambda}$. Doing a perturbative expansion, this ground state yields an effective Lagrangian which is invariant under $SU(3)_c \times U(1)_{em}$. The factor $U(1)_{em}$ is a combination of $U(1)_Y$ generator and the diagonal generator of $SU(2)_L$ and it is the gauge group of electromagnetism. If we write down the Lagrangian including this expansion, it would look rather formidable. But fortunately, there exists a gauge where it looks rather simple. This gauge is called the Unitary gauge and is parametrized by $\xi \to \infty$. Choice of gauge does not change the Physics. The Lagrangian then looks like:

$$\begin{aligned}
L \;=\; & -\frac{1}{2}\left(\partial_\mu W_\nu^+ - \partial_\nu W_\mu^+\right)\left(\partial_\mu W_\nu^- - \partial_\nu W_\mu^-\right) \\
& + \frac{1}{4}g^2\mathrm{v}^2 W^+W^- - \frac{1}{4}\left(\partial_\mu Z_\nu - \partial_\nu Z_\mu\right)^2 + \frac{1}{8}\left(\frac{e}{sc}\right)^2 \mathrm{v}^2 Z^2 \\
& - \frac{1}{4}\left(\partial_\mu A_\nu - \partial_\nu A_\mu\right)^2 - -\frac{1}{4}\left(\partial_\mu G_\nu^a - \partial_\nu G_\mu^a\right)\left(\partial^\mu G^{\nu,a} - \partial^\nu G^{\mu,a}\right) \\
& + \frac{1}{2}\partial^\mu h \partial_\mu h - \frac{1}{2}\lambda\nu^2 h^2 - \frac{1}{2}g^2\left[\left(W^+.W^-\right)^2 - \left(W^+\right)^2\left(W^-\right)^2\right] \\
& - e^2\left[A^2\left(W^+.W^-\right) - \left(A.W^+\right)\left(A.W^-\right)\right] \\
& - c^2g^2\left[Z^2\left(W^+.W^-\right) - \left(Z.W^+\right)\left(Z.W^-\right)\right] \\
& - c^2g^2\left[Z^2\left(W^+.W^-\right) - \left(Z.W^+\right)\left(Z.W^-\right)\right] \\
& - ecg\left[2\left(A.Z\right)\left(W^+.W^-\right) - \left(A.W^-\right) - \left(Z.W^+\right)\left(A.W^-\right)\right] \\
& + ie\left[\partial^\mu A_\nu W_\mu^- W_{nu}^+ + \partial^\mu W^{-\nu} W_\mu^+ A_\nu + \partial^\mu W^{+\nu} A_\mu W_\nu^-\right] + h.c. \\
& + ie\left[\partial^\mu Z_\nu W_\mu^- W_{nu}^+ + \partial^\mu W^{-\nu} W_\mu^+ Z_\nu + \partial^\mu W^{+\nu} Z_\mu W_\nu^-\right] + h.c.
\end{aligned} \tag{11}$$

$$
\begin{aligned}
&-\frac{1}{4}g_s^2\left(G^a.G^c\right)\left(G^b.G^d\right)f^{abe}fcde-\frac{1}{2}g_s\left(\partial_\mu G_\nu^c-\partial_\nu G_\mu^c\right)G^{\mu,a}G^{nu,b}f^{abc}\\
&-\frac{\lambda v}{2}h^3-\frac{\lambda}{8}h^4+\left(\frac{e}{2sc}\right)^2vhZ^2+\frac{1}{2}g^2vhW^+.W^-+\frac{1}{4}g^2h^2W^+.W^-\\
&+\frac{1}{8}\left(\frac{e}{sc}\right)^2h^2Z^2-\frac{m_e}{v}\bar{e}eh-\frac{m_u}{v}\bar{u}uh-\frac{m_d}{v}\bar{d}dh\\
&+\bar{\nu}\left(i\not{\partial}\right)\nu+\bar{e}\left(i\not{\partial}\right)e+\bar{u}\left(i\not{\partial}-m_u\right)u+\bar{d}\left(i\not{\partial}-m_d\right)d\\
&-\frac{g}{\sqrt{2}}\left(\bar{\nu}\not{W}^+\frac{(1-\gamma_5)}{2}e+\bar{u}\not{W}^+\frac{(1-\gamma_5)}{2}d+h.c.\right)+g_s\bar{u}\not{G}^a\frac{\lambda^a}{2}u+g_s\bar{d}\not{G}^a\frac{\lambda^a}{2}d\\
&+e\bar{e}\not{A}e+\frac{1}{3}e\bar{d}\not{A}d-\frac{2}{3}e\bar{u}\not{A}u-\frac{1}{4}esc\bar{\nu}\not{Z}\left(1-\gamma_5\right)\nu+\frac{1}{4}\frac{e}{sc}\bar{e}\not{Z}\left(1-s^2-\gamma_5\right)e\\
&-\frac{1}{4}\frac{e}{sc}\bar{u}\not{Z}\left(1-\frac{8}{3}s^2-\gamma_5\right)u+\frac{1}{4}\frac{e}{sc}\bar{d}\not{Z}\left(1-\frac{4}{3}s^2-\gamma_5\right)d
\end{aligned}
$$

The parameters e, s, c that appear in (11) are combination of parameters in the unbroken Lagrangian. Of these, s and c are the abbreviations, for $\sin\Theta_w$ and $\cos\Theta_w$ respectively, and

$$\tan\Theta_w \equiv \frac{g}{g'} \tag{12}$$

$$e = g\sin\Theta_w = g\cos\Theta_w \tag{13}$$

The mass of a fermion is given by

$$m_f = f\mathrm{v}/\sqrt{2} \tag{14}$$

The masses of the W , Z and the Higgs boson are

$$M_W^2 = \frac{1}{4}g^2\mathrm{v}^2 \tag{15}$$

$$M_Z^2 = \frac{1}{4}\frac{g^2\mathrm{v}^2}{c^2} \tag{16}$$

$$m_H^2 = \lambda\mathrm{v}^2 \tag{17}$$

The vacuum expectation value v is directly related to the Fermi constant, the effective strength of low-energy weak interactions, which is defined as

$$\frac{G_F}{\sqrt{2}} = \frac{g^2}{8M_W^2} \tag{18}$$

Experimentally, v=246 Gev.

The Physical states of photon and Z, which arise due to the fact that the mass matrix of physical fields are diagonal, are defined by

$$A^\mu \equiv \sin\Theta_w W_3^\mu + \cos\Theta_w B^\mu \tag{19}$$

$$Z^\mu \equiv \cos\Theta_w W_3^\mu - \sin\Theta_w B^\mu \tag{20}$$

Here, we have written in terms of only one generation of fermions . Generalization in terms of three generation is simple . We need to replace u, d, e, v by their counter parts in the other generations and add those terms in the Lagrangian.

The fermions acquire mass after symmetry breaking , and, by definition the mass matrices of Physical particles must be diagonal. The lepton sector can be diagonalized by simple redefinition since the neutrinos are massless. However, the quark sector introduces off diagonal terms in the couplings of the quarks to $W^\pm$ boson. That is, the charged current interaction of quarks becomes:

$$L_{cc} = \frac{g}{2}\overline{U}\not{W}^+\frac{1-\gamma_5}{2}VD_+ + h.c. \tag{21}$$

where V is a unitary 3×3 matrix,the Kobayashi-Maskawa(KM)[5] mixing matrix. The matrix looks like:

$$\begin{pmatrix} V_{ud} & V_{us} & V_{ub} \\ V_{cd} & V_{cs} & V_{cb} \\ V_{td} & V_{ts} & V_{tb} \end{pmatrix} \tag{22}$$

This matrix is roughly diagonal, each quark couples strongly to its partner in the same generation. All the elements are not necessarily real. The most general KM matrix can be parametrized by three real angles and one phase factor. There are experimental bounds on these elements . However, the phase is not well measured. A nonzero value of the phase explains the CP violation in the K meson system.

Shortcomings of the Standard model

Despite the successes of the Standard Model, there exist lots of unresolved issues. Mostly, they can be grouped into three broad categories: Problems of the gauge

sector, problems of the Yukawa sector, problems of the scalar sector.

The most serious objection with the gauge sector is it's arbitrariness. There are three unrelated coupling constatnts. Standard Model does not speak about their relative magnitudes.

The Standard Model does not provide any theoretical understanding as to why the fermion replicated in three generations. The $U(1)$ quantum number assigned to them is rather arbitrary. Moreover, the Standard Model does not say why the electric charged is quantized. Although it has been known for decades that weakly charged currents only couple to the left-handed fermions, the Standard Model provides no explanation for this symmetry.The fermion masses and the KM matrix element are completely arbitrary. Everybody wonders why the fermions differ in masses so much even in one generation.

The problems in the scalar sector is even more serious. The Standard Model relies on elementary scalars, the complex doublet Φ ,to break $SU(2)_L \times U(1)_Y$ symmetry. Theories with self interacting scalar fields usually suffer from two inherent problems known as naturalness and triviality.

The problem with naturalness deals with the scalar mass renormalization, which is quadratic in high-energy cut off. If an elementary scalar is much lighter than the cutoff, its mass is then the difference of two very large numbers. This situation is not only unnatural, requiring an extraordinarily precise cancellation, but it is also unstable under higher-order corrections. Just as naturalness is related to the mass renormalization of scalar fields, triviality is similarly related to coupling constant renormalization. The simple one-loop β function for the scalar self interaction given in Eqn.(3)

$$\mu \frac{d\lambda}{d\mu} = \frac{3}{4\pi^2}\lambda^2 \tag{23}$$

has the solution

$$\lambda(\mu) = \frac{1}{\lambda^{-1}(\mu_0) - \frac{3}{4\pi^2}\ln\left(\frac{\mu}{\mu_0}\right)} \tag{24}$$

which diverges at a finite energy scale. If this one-loop result is to be trusted, then the only way for a scalar field theory to be valid for all energy scales is when the coupling constant vanishes exactly.

Although these scalar theories are not valid in all scales , they can be regarded as effective theories that describe interactions at energies less than some scale Λ, where Λ is less than the scales at which scalar coupling constant would diverge . The larger the scalar self-interaction λ, the lower must be the scale Λ at which the new physics appears. Since λ is related to the mass of the Higgs boson, it implies that a heavy Higgs boson requires new physics at low scale.
Thus, all these doubts suggest that the SM is probably incomplete, and may, at some high energy scale Λ, be embedded in a more complete theory.

Extensions of the Standard Model

In order to tackle one or more issues discussed above, many different extensions of the Standard Model have been proposed . Since symmetry is the basic demand , many of these extensions involve symmetries beyond the $SU(3)_c \times SU(2)_L \times U(1)_Y$ gauge symmetry of the Standard Model.
In this thesis, effects of three possible extensions are discussed: extension of the flavor sector, extension of the color sector, extension of the theory to supersymmetric theories[6,7] where bosons and fermions are kept in the same irreducible representation involveing non-trivial extensions of the Poincare' group.
We would extend the flavor sector in two ways 1) inclusion of another abelian gauge group $U(1)$. The generator corresponds to an extra Z boson which cannot be ruled out by any experimental data. The presence of this boson may be justified from the viewpoint of Grand Unified Theory . It is almost a common view that the gauge couplings are unified at a common point at some high scale and the group which dictates the physics up there in the energy scale is a much bigger group which embeds the Standard model gauge group.In most of the cases, it is found that the bigger group has a subgroup $U(1)$ in addition to the Standard Model gauge group

$SU(3)_c \times SU(2)_L \times U(1)_Y$. For example, popular unifying groups like $SO(10)$, E_6[8] etc. 2)We also extend the flavor sector by enlarging $SU(2)_L$ to $SU(3)_L$ [9] . The interesting effect is justification for the existence of three families. Standard Model never provides any reason for the existence of three families.

We extend the color sector for the third generation from $SU(3)_c$to $SU(3) \times SU(3)$ at some high scale[10]. This product group spontaneously breaks down to normal $SU(3)_c$ .The reason for treating the third generation in a different way is the presence of heaviest fermions and the large production cross-section for the top quark. In this model, one can also produce a condensation mechanism for the production of Higgs which justifies the existence of this no longer elementary scalar boson.

If proven to be true, existence of Supersymmetry would be the most intriguing discovery of Particle physics. Though the particles predicted by this symmetry is yet to be seen, the potential of this symmetry to solve various unsolved problems in Standard Model is remarkable. It solves the naturalness problem , it unifies the gauge couplings at a fixed point. Local version of this symmetry involves gravity. Of late, people are trying to solve QCD from this symmetry view point.

CHAPTER II

EXTENSION OF THE FLAVOR SECTORS

Introduction

The Standard Model i.e. SU(2)×U(1) gauge theory of the weak and electromagnetic interactions is in excellent agreement with the present experimental data. However, the possibility of an extra chiral U(1) is never ruled out. In fact, its existence can be explained naturally in most of the Grand Unified Theories. Presence of this extra group introduces lots of new parameters e.g. a new gauge coupling, new hypercharges for the fermions and Higgs, vevs for the new Higgs. So, some more observables are required in the theory. These could be the two new angles, mass of extra Z, additional ρ parameter etc. The standard procedure is to diagonalize Z Z' mixing matrix assuming the existence of photon there and thereby producing a relation between M_2 and the new mixing angle ϕ. Stringent bound on ϕ can be obtained from the GUT theory. In this chapter, we develop a formalism to determine the photon eigenstate elegantly along with Z_1 and Z_2 in the most general case, we also reflect on how the contribution of this extra U(1) to the electromagnetic charge actually determines the Higgs sector. In the end, we discuss a specific model where the fermions do not couple to the extra Z boson. The theories in which the extra Z boson does not couple to the fermions, the usual production and decay signatures of Z fails. We discuss the production and decays of such a Z via the W^+W^- mode, and also delineate how the presence of such a Z boson may affect the detection of the Higgs boson of comparable mass.

Masses and Mixing Angles

The existence of three neutral gauge bosons with one Higgs scalar in the theory leads us to the most general 3×3 mass matrix of the form

$$M^2 = aa^T \tag{25}$$

with a being the 3-d real vectors. This can be generalized for n scalars as

$$M^2 = aa^T + bb^T + cc^T + \cdots \tag{26}$$

where a, b, c,$\cdots$ are 3-d real vectors. Additional terms like $(a^Tb+b^Ta+\cdots)$ can always be absorbed in the redefinition of a,b,c. Now, we claim that in order to have 0 eigenvalue for M, all the vectors but two will be linearly dependent. To prove that, let us start with 3 independent vectors.

Assuming a,b,c are linearly independent vectors, the photon vector has the general form :

$$k = u(a \times b) + v(b \times c) + w(c \times a) \tag{27}$$

Since $M^2k = 0$, which implies $u = v = w = 0$, there is no photon eigenvector in the theory.

On the otherhand, if we assume a,b and c are three linearly dependent vectors spanning a 2d space, then we can write $M^2 = aa^T + bb^T$ with a and b as linearly independent. The most general eigenvector in this case is $k = u(a \times b) + vb + wa$. Assuming a and b are linearly independent, it can be shown that $v = w = 0$, having photon as one of our eigenvectors.

If we have a,b,c span the 1-d space, we can then write without loss of generality $M^2 = aa^T$ which implies that we have two photons.

The most general 3×3 real symmetric matrix with one 0 eigenvalue and two non-zero ones can be written as

$$M^2 = aa^T + bb^T \tag{28}$$

with the photon vector given by $e_0 = a \times b$. The other eigenvectors and eigenvalues are most easily obtained in the 2-D subspace orthogonal to e_0 in the a-b basis in

which M takes on the form

$$M^2 = \begin{bmatrix} (a\cdot a) & (a\cdot b) \\ (a\cdot b) & (b\cdot b) \end{bmatrix} \tag{29}$$

where $(a\cdot b)$ gives the mixing term. We also find the usual mass relation:

$$\tan^2\lambda = \frac{(a\cdot a)-m_1^2}{m_2^2-(a\cdot a)} = \frac{m_2^2-(b\cdot b)}{(b\cdot b)-m_1^2} \tag{30}$$

The usual practice is to write m_0^2 (the SM z mass) instead of $(a\cdot a)$.If a and b are orthogonal to each other from the beginning, then a and b are the eigenvectors of M with eigenvalues $m_1^2=(a\cdot a)$ and $m_2^2=(b\cdot b)$ and they give masses to Z_1 and Z_2.

While this is the simple way to get the eigenvalues, the direction of the eigenvectors in the original 3-dim space needs to be known. We represent the $U(1)_Y$,$SU(2)_L$ and $U(1)_{Y'}$ directions with (x,y,z).The two angles θ and ϕ for defining photon vectors are given by:

$$\tan\theta \equiv \frac{\sqrt{(a\times b)_y^2+(a\times b)_z^2}}{(a\times b)_x}, \qquad \tan\phi \equiv \frac{(a\times b)_z}{(a\times b)_y} \tag{31}$$

Then, the normalized photon vector is given by

$$|\gamma\rangle = \begin{bmatrix} \cos\theta \\ \sin\theta\cos\phi \\ \sin\theta\sin\phi \end{bmatrix} \tag{32}$$

As soon as the photon vector gets defined, the matrix M gets blockdiagonal with a 2×2 non-diagonal block . The rotation that has to be operated on the matrix to achieve this can be written as U^{-1}=$R_x(\phi)R_z(\theta)$ .To make the matrix completely diagonal, we need another rotation which can be a rotation about the x axis given by $R_x(\psi)$. The final vectors z_1 and z_2 can be written as

$$\begin{aligned} |z_1\rangle &= \begin{bmatrix} -\sin\theta\cos\psi \\ \cos\theta\cos\phi\cos\psi-\sin\phi\sin\psi \\ \sin\phi\cos\theta\cos\psi+\cos\phi\sin\psi \end{bmatrix}, \\ |z_2\rangle &= \begin{bmatrix} \sin\theta\sin\psi \\ -\cos\theta\cos\phi\sin\psi-\sin\phi\cos\psi \\ -\sin\phi\cos\theta\sin\psi+\cos\phi\cos\psi \end{bmatrix}. \end{aligned} \tag{33}$$

Higgs-Sector

So far, we have not yet specified the Higgs structure of this theory. At this point, let us write a,b as:

$$a = \begin{bmatrix} g'Y_a \\ gI_{3a} \\ g''Y'_a \end{bmatrix} v_a, \qquad b = \begin{bmatrix} g'Y_b \\ gI_{3b} \\ g''Y'_b \end{bmatrix} v_b, \tag{34}$$

where v_a and v_b are the Higgs VEVs. Using our prescription, one can easily find the photon vector, as well as Z_1, Z_2. For the photon vector, we have in terms of the components of a and b:

$$e_0 = \begin{bmatrix} a_y b_z - b_y a_z \\ a_z b_x - a_x b_z \\ a_x b_y - a_y b_x \end{bmatrix} \tag{35}$$

If the introduction of the extra U(1) does not affect the photon vector, i.e., the definition of charge remain unchanged, then the 3rd component of the photon vector becomes 0. This gives rise to two interesting scenarios: 1.b_x=b_y=0, if we also assume a_z=0 we have $a \cdot b$=0 which means $(a \cdot a)$=m_1^2, $(b \cdot b)$=m_2^2 ,so $\tan\lambda$=0. However, if a_z is not 0 , there is mixing, and $(a \cdot a)$ is $(g^2 + g'^2Y_a^2 + g''^2Y_a'^2)v_a^2/4$, but for $(a \cdot a)$ the common lore is to use the SM Z mass which is predicted by the w mass. 2. b_x, $b_y \neq 0$ then we get a condition:

$$\frac{b_x}{a_x} = \frac{b_y}{a_y} \neq 0 \tag{36}$$

in this case $(a \cdot a)$ is $(g^2 + g'^2Y_a^2 + g''^2Y_a'^2)v_a^2/4$ which is again not the usual SM Z mass. It reduces to $m_0^2 \cos^2\beta$ ($\tan\beta$=$\frac{v_b}{v_a}$) in some approximation.

Anomaly Cancellation

Here, we address the problem of anomaly cancellation. We will only look at a single generation of fermions whose $SU(2)_L \times U(1)_Y \times U(1)_{Y'}$ quantum number assignments we write as:

$$q_L = \begin{bmatrix} u_L \\ d_L \end{bmatrix} = (2, Y_q, Y'_q), \qquad \ell_L = \begin{bmatrix} \nu_L \\ e_L \end{bmatrix} = (2, Y_\ell, Y'_\ell). \tag{37}$$

for the left–handed fermions and

$$u_R = (1, Y_u, Y'_u), \quad , d_R = (1, Y_d, Y'_d), \quad e_R = (1, Y_e, Y'_e) \tag{38}$$

for the right–handed fermions.

The anomaly conditions are given by:

- $[SU(3)]^2U(1)_Y$ and $[SU(3)]^2U(1)_{Y'}$:

$$\begin{aligned} 2Y_q &= Y_u + Y_d, \\ 2Y'_q &= Y'_u + Y'_d. \end{aligned} \tag{39}$$

- $[SU(2)_L]^2U(1)_Y$ and $[SU(2)_L]2U(1)_{Y'}$:

$$\begin{aligned} 3Y_q &= -Y_\ell \\ 3Y'_q &= -Y'_\ell. \end{aligned} \tag{40}$$

- $[U(1)_Y]^3$ and $[U(1)_{Y'}]^3$:

$$\begin{aligned} 6Y_q^3 - 3Y_u^3 - 3Y_d^3 + 2Y_\ell^3 - Y_e^3 &= 0 \\ 6Y_q'^3 - 3Y_u'^3 - 3Y_d'^3 + 2Y_\ell'^3 - Y_e'^3 &= 0 \end{aligned} \tag{41}$$

- $[U(1)_Y]^2U(1)_{Y'}$ and $U(1)_Y[U(1)_{Y'}]^2$:

$$\begin{aligned} 6Y_q^2Y'_q - 3Y_u^2Y'_u - 3Y_d^2Y'_d + 2Y_\ell^2Y'_\ell - Y_e^2Y'_e &= 0 \\ 6Y_qY_q'^2 - 3Y_uY_u'^2 - 3Y_dY_d'^2 + 2Y_\ell Y_\ell'^2 - Y_eY_e'^2 &= 0 \end{aligned} \tag{42}$$

- Gravitational anomaly:

$$\begin{aligned} 6Y_q - 3Y_u - 3Y_d + 2Y_\ell - Y_e &= 0 \\ 6Y'_q - 3Y'_u - 3Y'_d + 2Y'_\ell - Y'_e &= 0 \end{aligned} \tag{43}$$

In addition to these conditions, we require that the left and right–handed fermions get the same electromagnetic charge:

$$\frac{1}{2} + pY_q + qY'_q = pY_u + qY'_u = Q_u,$$

$$\begin{aligned} -\frac{1}{2} + pY_q + qY'_q &= pY_d + qY'_d = Q_d, \\ -\frac{1}{2} + pY_\ell + qY'_\ell &= pY_e + qY'_e = Q_e. \end{aligned} \tag{44}$$

It is relatively easy to show that these conditions imply electromagnetic charge quantization, i.e.:

$$Q_u = \frac{2}{3}, \quad Q_d = -\frac{1}{3}, \quad Q_\nu = 0, \quad Q_e = -1. \tag{45}$$

Now, it turns out that all these conditions can be met by simply taking all the Y_X's and Y'_X's to be proportional to the usual hypercharges. For instance,

$$\begin{aligned} &Y_q = \tfrac{A}{6p}, \quad Y_u = \tfrac{2A}{3p}, \quad Y_d = -\tfrac{A}{3p}, \quad Y_\ell = -\tfrac{A}{2p}, \quad Y_e = -\tfrac{A}{p}, \\ &Y'_q = \tfrac{B}{6q}, \quad Y'_u = \tfrac{2B}{3q}, \quad Y'_d = -\tfrac{B}{3q}, \quad Y'_\ell = -\tfrac{B}{2q}, \quad Y'_e = -\tfrac{B}{q}, \end{aligned} \tag{46}$$

with $A + B = 1$ is obviously a solution. Actually, it is possible to prove that this is the only solution.

Next, consider introducing a right–handed neutrino into our theory:

$$\nu_R = (1, Y_\nu, Y'_\nu). \tag{47}$$

The anomaly cancellation conditions that are modified are:

- $[U(1)_Y]^3$ and $[U(1)_{Y'}]^3$:

$$\begin{aligned} 6Y_q^3 - 3Y_u^3 - 3Y_d^3 + 2Y_\ell^3 - Y_e^3 - Y_\nu^3 &= 0 \\ 6Y_q'^3 - 3Y_u'^3 - 3Y_d'^3 + 2Y_\ell'^3 - Y_e'^3 - Y_\nu'^3 &= 0 \end{aligned} \tag{48}$$

- $[U(1)_Y]^2 U(1)_{Y'}$ and $U(1)_Y [U(1)_{Y'}]^2$:

$$\begin{aligned} 6Y_q^2 Y'_q - 3Y_u^2 Y'_u - 3Y_d^2 Y'_d + 2Y_\ell^2 Y'_\ell - Y_e^2 Y'_e - Y_\nu^2 Y'_\nu &= 0 \\ 6Y_q Y_q'^2 - 3Y_u Y_u'^2 - 3Y_d Y_d'^2 + 2Y_\ell Y_\ell'^2 - Y_e Y_e'^2 - Y_\nu Y_\nu'^2 &= 0 \end{aligned} \tag{49}$$

- Gravitational anomaly:

$$\begin{aligned} 6Y_q - 3Y_u - 3Y_d + 2Y_\ell - Y_e - Y_\nu &= 0 \\ 6Y'_q - 3Y'_u - 3Y'_d + 2Y'_\ell - Y'_e - Y'_\nu &= 0 \end{aligned} \tag{50}$$

We also require that left and right-handed neutrinos to have the same electromagnetic charge:

$$\frac{1}{2} + pY_\ell + qY'_\ell = pY_\nu + qY'_\nu = Q_\nu. \tag{51}$$

This time, these conditions are not sufficient to determine the electromagnetic charges. Thus, we must assume $Q_\nu = 0$.

Now, obviously, Eq. (46) with $Y_\nu = Y'_\nu = 0$ is a solution to these conditions. But since we have an extra degree of freedom, one might think, that there must be other solutions as can be found in $SO(10)$ GUT derived models. Then, the natural question is: What is the most general solution to these conditions? Is there a simple way of parameterize the different solutions? Can it interpolate between all known solutions from GUT models?

One may try in the following way to answer to these questions:

$$\begin{array}{lll} Y_q = \frac{A}{6p} - \frac{C}{3p} & Y_u = \frac{2A}{3p} - \frac{C}{3p} & Y_d = -\frac{A}{3p} - \frac{C}{3p} \\ Y_\ell = -\frac{A}{2p} + \frac{C}{p} & Y_\nu = \frac{C}{p} & Y_e = -\frac{A}{p} + \frac{C}{p} \\ Y'_q = \frac{B}{6q} - \frac{D}{3q} & Y'_u = \frac{2B}{3q} - \frac{D}{3q} & Y'_d = -\frac{B}{3q} - \frac{D}{3q} \\ Y'_\ell = -\frac{B}{2q} + \frac{D}{q} & Y'_\nu = \frac{D}{q} & Y'_e = -\frac{B}{q} + \frac{D}{q} \end{array} \tag{52}$$

where $A + B = 1$ and $C + D = 0$.

All the $SO(10)$ derived models can be parameterized in this way. If they can, then we can write J_Y and $J_{Y'}$ as

$$\begin{aligned} pJ_Y &= A(J_Q - J_3) - CJ_{B-L}, \\ qJ_{Y'} &= B(J_Q - J_3) - DJ_{B-L}. \end{aligned} \tag{53}$$

This, in turn, will let us write J_Z and $J_{Z'}$ in terms of J_Q, J_3, and J_{B-L}.

We have three different kinds of models χ, Ψ, and η. These models occur in the following breaking:

χ $SO(10) \to SU(5) \times U(1)_\chi$.

ψ $E_6 \to SO(10) \times U(1)_\psi$.

η $E_6 \to$ rank 5 group in Superstring inspired models.

Only the case χ lets us write

$$2\sqrt{10}Q_\chi = 4(J_3 - J_Q) - 5J_{B-L}. \tag{54}$$

However, the charges Q_ψ and Q_η do not satisfy the anomaly cancellation conditions that we wrote down, because they have more than 15 fermions to begin with.

Extra Z without fermion coupling

Most of the theoretical and experimental work in looking for such an extra Z boson have been done in the context of the superstring motivated $E6$ models[11]. In all such models, the extra Z boson couples to both the fermions and the weak gauge bosons. In both the leptonic and hadronic colliders, such gauge boson is produced via its coupling to the fermions; while the easiest decay mode for its detection is its decay to a pair of charged leptons. The hadronic collider bounds on its mass comes from these modes. The extra Z boson can also mix with the standard model (SM) Z, and thus affect the mass of the SM Z. Thus, interesting bound on the mass of the extra Z and its mixing angle Φ with the SM Z comes from the accurate measurement of the Z-mass and determines how different it is from the SM prediction. Combining all the available data, the current bound on the mass and mixing angle for the extra Z in the E6 models is $170 - 350GeV$ and 0.02 [12–16]. In this work[17], we consider a different class of models with an extra $U(1)$ in which the Z boson does not couple directly to the fermions. Such models are easily constructed by choosing the hypercharge of the fermions with respect to the extra $U(1)$ to be zero. Such a Z'(Z' is the current eigenstate and the Z_2 is the mass eigenstate) could still couple to the ordinary fermions via its mixing with Z. But, since the mixing angle is very small, its production via the ordinary fermions in leptonic and hadronic colliders will be very much suppressed. For the same reason, its decay into ordinary fermions will also be very small. The most important production and decay mode of such a Z will be via its coupling to W^+W^- pair. The coupling to pair W^+W^- is also suppressed by the same mixing Φ. However, both the production and decay now is proportional to extra higher powers of $\left(\frac{M_{Z_2}}{m_w}\right)^8$ and $\left(\frac{M_{Z_2}}{m_w}\right)^8$ compared to the production and decay respectively via

the fermionic mode. As a result, W^+W^- will be the most dominant production and decay mode of such an extra Z boson. Below, we consider the production of Z_2 at resonance via the W^+W^- mode and its decay to W^+W^- pair, as well as compare the production and decay of the standard model Higgs boson via the same mode. The differential cross section for the process $W^+W^- \to W^+W^-$ via the s-channel Z_2 exchange is obtained to be

$$\frac{d\sigma}{d(\cos\theta)} = \frac{\mid M \mid^2}{32\pi s} \tag{55}$$

where the spin-averaged matrix element squared, $\mid M \mid^2$is

$$\begin{aligned} \mid M \mid^2 \;=\; & \frac{16g^4 \cos^2\theta_w \sin^2\Phi}{9[(s-M^2)^2+\Gamma^2M^2]}\frac{E^{12}}{m^8} \times (16n^2+64x \\ & -64n^2x+120n^2x^2-144x^3+136n^2x^3+32x^4+97n^2x^4 \\ & +48x^5-42n^2x^5+9n^2x^6) \end{aligned} \tag{56}$$

Here, M and m are the masses of the Z_2 and W boson respectively, E is the energy of each W boson in the center of mass frame,Γ , is the total width of Z_2,Φ is the scattering angle in the center of mass frame, $s = 4E^2$. There are also contributions to the process due to s and t channel γ and Z exchanges and also due to t channel Z_2 exchanges. Since we are interested only on or near the Z_2 resonance, these contributions are negligibly small. There are also contributions from the Higgs boson exchanges which we shall discuss shortly. From Eq. (55), the total cross section on or near the Z resonance is

$$\sigma = \frac{g^4 \cos^2\theta_w \sin^2\Phi}{27\pi s[(s-M^2)^2+\Gamma^2M^2]}\frac{E^{12}}{m^8} \times (16+128x+120x^2-568x^3+193x^4+102x^5+9x^6) \tag{57}$$

The partial width for decay is given by

$$\Gamma(Z_2 \to W^+W^-) = \frac{g^4 \cos^2\theta_w \sin^2\Phi}{192\pi m^4} M^5 \times [(1-4y)^{3/2}(1+20y+12y^2)] \tag{58}$$

where $y \equiv (m^2/M^2)$. Using Eqs. (57) and (58), the total cross section on or near the resonance can be written as

$$\sigma(E) = \frac{16\pi}{3}\frac{M^2}{M^2-4m^2}\frac{[\Gamma(Z' -> WW)]^2}{(4E^2-M^2)^2+\Gamma^2_{total}M^2} \tag{59}$$

Eq. (59) agrees with the standard Breit-Wigner formulae. In the usual superstring motivated $E6$ models, Z' couples directly to the fermions, whereas it couples W^+W^- to only through the mixing with Z. Since the mixing angle is very small, it is atmost comparable to [18–20]. The enhancement factor $(M/m)^4$ is compensated by the suppression factor $\sin^2\Phi$. However, in the class of models we consider, since Z' does not couple directly to the fermions, both the processes $f_1\overline{f_1} \rightarrow Z_2 \rightarrow f_2\overline{f_2}$ and $W^+W^- \rightarrow Z_2 \rightarrow W^+W^-$ are suppressed by the mixing factor, $\sin^4\Phi$. However, the process has the extra enhancement factor $(M/m)^8$. As a result, extra Z production and decay via the mode dominate over the fermionic mode.

In Figs. 1,2 and 3 we plot the cross-sections, for the process against the center of mass energy, E_{cm} of the W^+W^- pair for $M = 400,\ 600, 800, 1,000, 1,200$ and $1,600GeV$. Although the current experimental bound on the mixing angles is $\sin\Phi = 0.02$, we have used $\sin\Phi = 0.01$ in a conservative manner. Had we used $\sin\Phi = 0.02$, the cross-sections would have been 16 times larger. As expected, because of the suppression $\sin^4\Phi$ coming from the mixing angle, the Z_2 peak is very narrow, and the cross-sections are very sharply peaked around M_{extraZ}. The fermionic decay widths, $Z_2 = ff$ is negligibly small, the total decay width is essentially due to $Z_2 = W^+W^-$. The values of the total width for the above Z_2 masses are $0.02, 0.13, 0.49, 1.44, 3.50$ and $14.4GeV$ respectively. The cross sections at the peak are quite large, $\sigma \cong 4.7 \times 10^4$ pb for $M = 400GeV$ whereas $\sigma \cong 2.8 \times 10^4$ pb for $M = 1600GeV$. For the same values of the Higgs boson masses, the corresponding values of the cross-sections for the process $W^+W^- \rightarrow H \rightarrow W^+W^-$ is also shown. As expected, the Higgs boson resonance is much wider than the Z_2, but as shown, the cross sections at the peak for the Z case is much larger. Thus, a detector with a very good resolution could easily see the Z_2 peak over the Higgs boson. In reality, the detectors will have a finite energy resolution. In the table I, we give the integrated values of the cross-sections $\left(\Sigma = \int_{E_1}^{E_2} \sigma(E)\, dE\right)$ for various detector resolutions $\Delta E = E_2 - E_1$. For small values of the Higgs or extra Z masses, say 400 GeV to 600 GeV, the Higgs integrated cross section is larger. For masses of 800 to 1000 GeV, the two cross sections are comparable for ΔE upto $20GeV$, whereas for $\Delta E > 20GeV$, the Higgs is still larger. For very

large masses, say 1,200 to 1,500 GeV, Z cross-sections are larger than the Higgs cross sections for upto ΔE upto $40GeV$. But for $\Delta E > 40\ GeV$, the two cross-sections ae comparable.

Detection of this Z

What will be the signal of such an Z_2 boson? Each of the final state W^+W^- pair will decay to a charged lepton and a neutrino. Thus, the signal will be a pair of oppositely charged lepton (say $\mu^+\mu^-$) together with the missing neutrinos. If the detector resolution for measuring the energies of the pair is very good, then we shall see a sharp peak in the energy distribution of the pair, which is the characteristic of the very sharp peak of Z_2. This will be a very clear signal of Z_2 over the Higgs boson. If the detector resolution is not very good, we shall still see a moderate peak (or excess pair) in the energy distribution around the half of the Z_2 mass. Whether this signal is due to a Z or a Higgs boson can be acertained from the angular distribution of the pair. In Fig. 4(a) and 4(b) we plot the angular distributions of the W^+W^- pair for the process for M_{Z_2}= 400, 600, 800, GeV and 1,000, 1,200, and 1,500 Gev. The corresponding angular distribution for the process is flat, which is the characteristics of the scalar nature of the Higgs boson. These two distributions would be reflected in the angular distributions of the ensuing pair. Thus, the presence of both a Higgs boson and an Z_2 with large and comparable masses (around 1 TeV) will confuse the Higgs signal. But it can be distinguished by studying the excess pairs and their angular distributions.

Extension of $SU(2)_L$ to $SU(3)_L$

Standard Model (SM) has several unsatisfactory features. For example, it cannot explain the repetation of the fermion families. Moreover, the possibility of a larger gauge group at the TeV scale is not excluded by the current data. Recently, Frampton[9], and also Pisano and Pleitz[21] have proposed a (331) model based on

TABLE I.

The integrated values of the cross-sections $\Sigma\,(10^{-5} pbGeV)$ for Z_2 and H resonance for various detector resolutions

M(GeV)		$\triangle E(GeV)$							
		6	10	20	40	60	80	100	200
400	$\sigma(Z')$	0.014	0.014	0.014					
	$\sigma(H)$	0.300	0.500	0.900					
600	$\sigma(Z')$	0.037	0.037	0.037					
	$\sigma(H)$	0.12	0.211	0.419					
800	$\sigma(Z')$	0.076	0.077	0.078	0.079				
	$\sigma(H)$	0.076	0.128	0.255	0.506				
1000	$\sigma(Z')$	0.125	0.134	0.144	0.144	0.144	0.145		
	$\sigma(H)$	0.05	0.086	0.164	0.343	0.513	0.678		
1200	$\sigma(Z')$	0.163	0.193	0.218	0.233	0.237	0.239		
	$\sigma(H)$	0.037	0.06	0.12	0.246	0.369	0.49		
1200	$\sigma(Z')$	0.156	0.227	0.320	0.390	0.417	0.429	0.437	0.458
	$\sigma(H)$	0.024	0.041	0.081	0.162	0.244	0.32	0.400	0.803

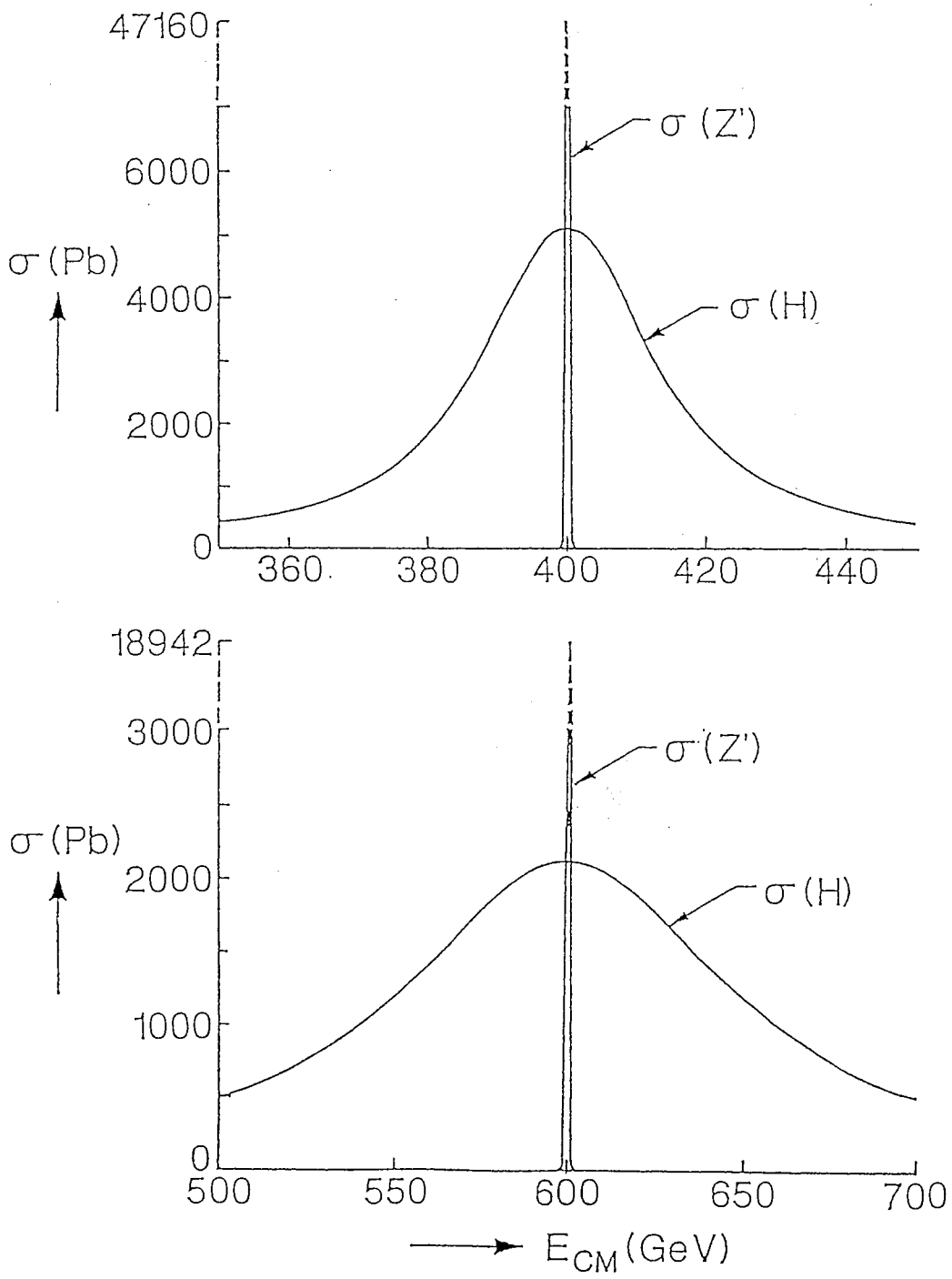

Figure 1. variation of the cross sections $\sigma(Z')$ and $\sigma(H)$with the W^+W^- center of mass energy E_{CM} for M =400,600 GeV.

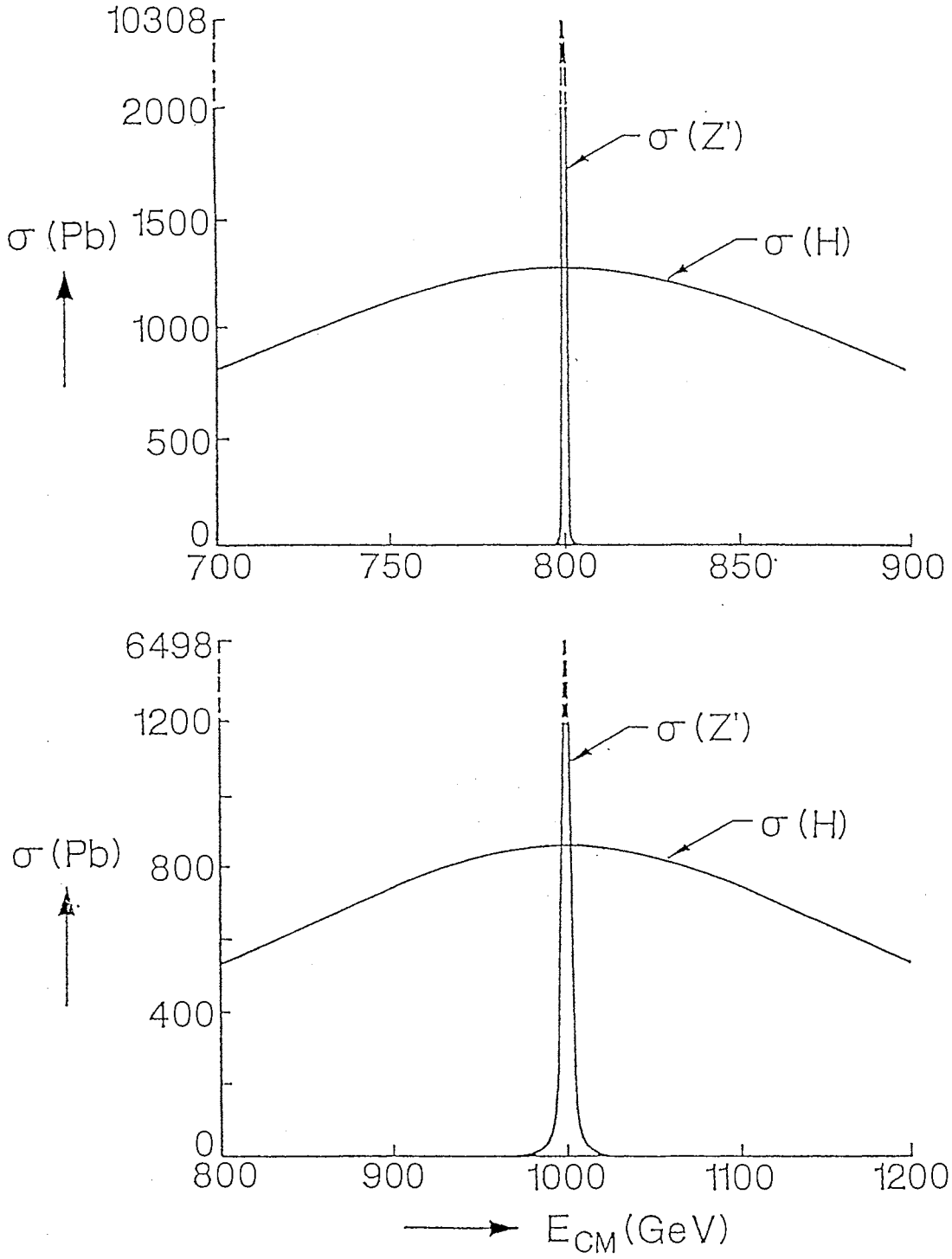

Figure 2. variation of the cross sections $\sigma(Z')$ and $\sigma(H)$with the W^+W^- center of mass energy E_{CM} for M =800,1000 GeV.

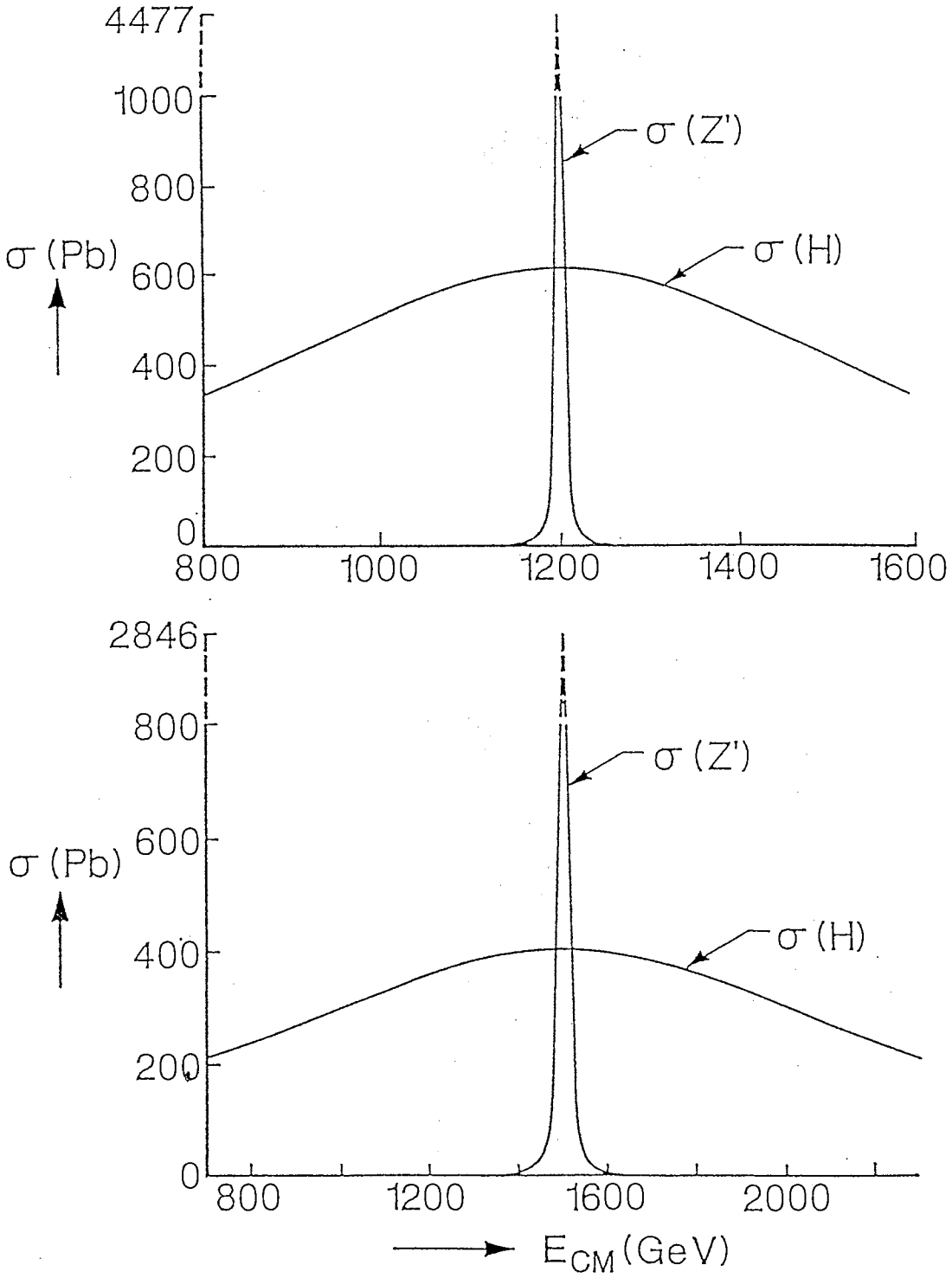

Figure 3. variation of the cross sections $\sigma(Z')$ and $\sigma(H)$with the W^+W^- center of mass energy E_{CM} for M =1200,1600 GeV.

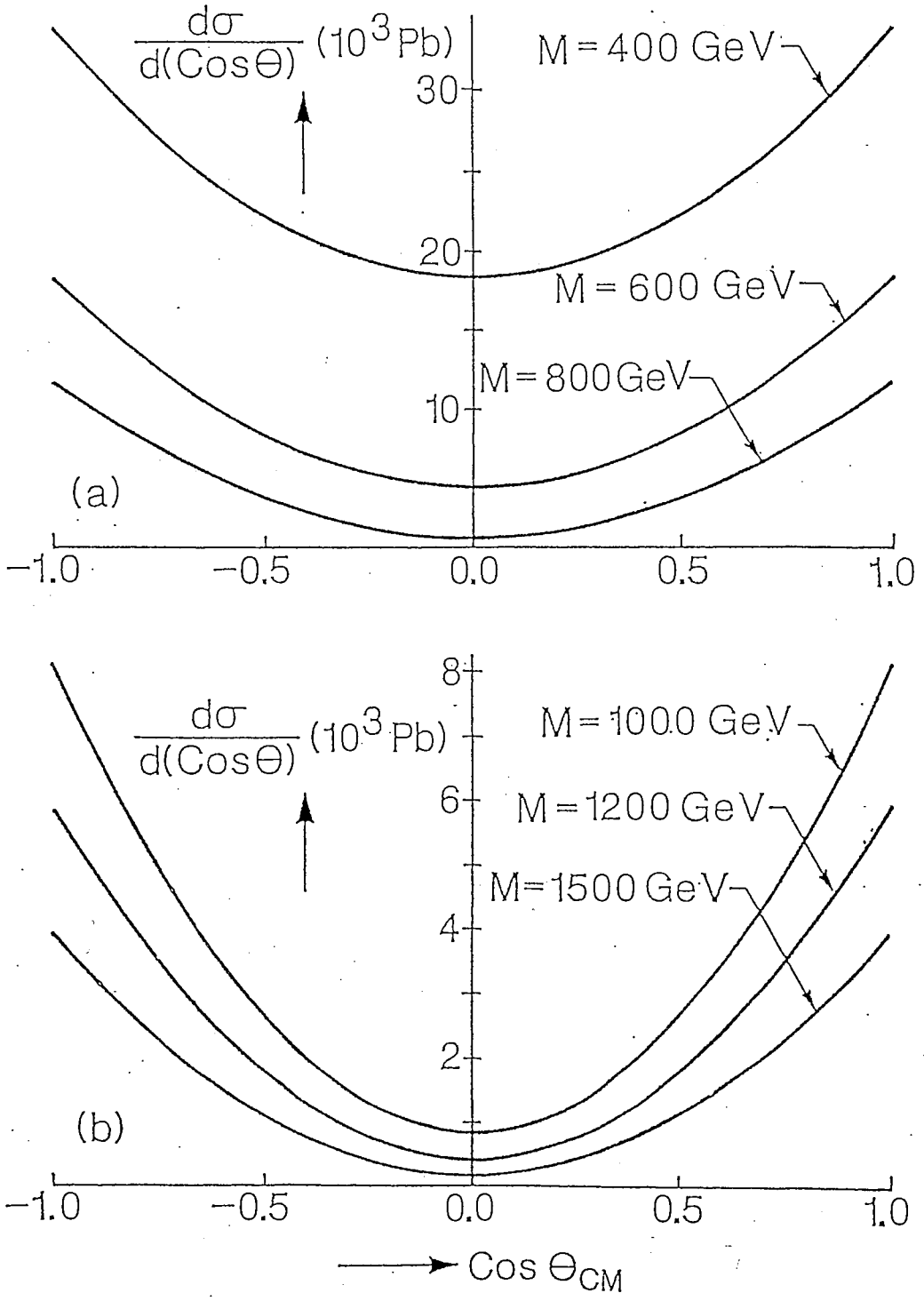

Figure 4. The angular distribution for M =400, 600,800 GeV and 100,1200,1600 GeV.

the extended gauge group $SU(3)_c \times SU(3)_L \times U(1)$. In this model, the gauge anomalies cancel among the three families (and is crucially dependent on the existence of three colors) thereby giving a reason why we need three families. One very interesting feature of this model is that it has dilepton gauge bosons, $Y^{++}$and Y^{--} which couple both to two quarks and two leptons. Doubly charged dileptons (Y^{++}, Y^{--}) are also present in the $SU(15)$ gauge model[22–24]. But in that scheme, such dileptons are exchanged only between the leptons because the fermionic multiplet 15 contains the SM quarks and antiquarks only. Hence, these dileptons 1 in the $SU(15)$scheme can not be produced directly in hadron colliders. In the (331) model, three lepton families are assigned to 3_L^* of $SU(3)_L$.

$$3_l^* = \begin{pmatrix} e^- \\ \vartheta_e \\ e^+ \end{pmatrix}, \begin{pmatrix} \mu^- \\ \vartheta_\mu \\ \mu^+ \end{pmatrix}, \begin{pmatrix} \tau^- \\ \vartheta_\tau \\ \tau^+ \end{pmatrix}$$

For the first two families, the assignment of the quarks under $SU(3)_l$ are as follows:
1st family:

$$3_L = \begin{pmatrix} u \\ d \\ D \end{pmatrix}_L, (u^c)_L, (d^c)_L, (D^c)_L$$

2nd family:

$$3_L = \begin{pmatrix} c \\ s \\ S \end{pmatrix}_L, (c^c)_L, (s^c)_L, (S^c)_L$$

Here, D and S are two new $SU(2)_L$ singlet quarks with charges -4/3. The 3rd family is assigned to antitriplet and singlets of $SU(2)_l$.

3rd family:

$$3_L^* = \begin{pmatrix} b \\ t \\ T \end{pmatrix}_L, (b^c)_L, (t^c)_L, (T^c)_L$$

The new $SU(2)_L$ singlet quark, T has electric charge $= -4/3$. The chiral anomalies get cancelled between the three families which provides a reason for having

3 families. The gauge bosons, Y^{--}, Y^{-} have lepton number +2, while Y^{++}, Y^{+} have lepton number -2. The 331 model does not conserve separate family lepton numbers, $Li(i = e, \mu, \tau)$, but the total lepton number, $L = L_e + L\mu + L_\tau$ is conserved. The exotic quarks D and S have $L = +2$ while T has $L = -2$. The 331 symmetry is broken to the SM by using a $SU(3)_l$. Higgs triplet with VEV $< \Phi^c >= U\delta^{c3}$. This gives masses to the new quarks D, S, T as well as the gauge bosons $Y^{\pm\pm}$, $Y^{\pm}$ and Z'.

Productions of Dilepton gauge bosons

We calculate the cross-sections[25] for the productions of the dilepton gauge bosons (Y^{++}, $Y^{--}, Y^{\pm}$) in hadron colliders such as Fermilab Tevatron or LHC. The dominant mechanism is the associated production of Y's with the exotic quarks D or S via the quark gluon fusion. The diagrams for the processes

$$u + g = Y^{++} + D, \overline{u} + g = Y^{--} + \overline{D}$$

$$d + g = Y^{+} + D, \overline{d} + g = Y^{-} + \overline{D}$$

are shown in Fig.5. For simplicity, we assume that the exotic quarks S and T are much heavier, and only D is being produced at these energies. The cross-section for the subprocess $q + g \rightarrow Y + D$ is obtained to be

$$\frac{d\sigma}{dt} = \frac{\pi\alpha\alpha_s}{48s^2 \sin^2\Theta_w} T(s, t, m, M) \tag{60}$$

where

$$\begin{aligned} T(s,t,m,M) \;=\; & \frac{8}{s^2}\left(\frac{m^4 s}{M^2} - 2\frac{m^2 s^2}{M^2} - \frac{M^2 st}{M^2} + \frac{s^3}{M^2} + \frac{s^2 t}{M^2} + 2m^2 s\right. \\ & \left. -s^2 - 2st\right) + \frac{16}{s\,(t - m^2)}\left(-2M^4 + M^2 m^2\right. \\ & +2M^2 m^2 + 2M^2 m^2 + 2M^2 s + 2M^2 t - \frac{m^4 t}{M^2} \\ & \left. +2\frac{m^2 st}{M^2} - \frac{s^2 t}{M^2} - \frac{st^2}{M^2} + m^4 - m^2 t + st\right) \\ & + \frac{4}{(t - m^2)^2}\left(4m^2 M^2 + \frac{m^4 t}{M^2} - \frac{m^2 st}{M^2} + 4\frac{m^2 t^2}{M^2}\right. \\ & \left. + \frac{st^2}{M^2} + \frac{t^3}{M^2} - M^4 + 2m^2 s - 2st - t^2\right) \end{aligned} \tag{61}$$

where and $m = M_D$, $M = M_Y$. The total cross section, σ for the process $P + P \rightarrow Y + D+$ anything or $P + P \rightarrow Y + D +$ anything is obtained by first integrating over t, and then folding the appropriate parton distributions:

$$\sigma = \int \frac{dL}{d\tau}\sigma(s, m, M)dt \tag{62}$$

Here σ is the cross section for the subprocess given by 60, and s is the center of mass energy for the quark- gluon system. We note that the variables s, t given in eq. (1) are appropriate for the subprocess, namely these are s and t. The luminosity function $dL/d\tau$ is given by

$$\frac{dL}{d\tau} = \int_\tau^1 f_i(x)f_j(x)\frac{dx}{x}$$

where $f_i(x)$ are the distribution functions of the appropriate quarks or gluons in the proton or antiproton. We have used the distribution functions produced by the $CTEQ$ collaboration at $Q^2 = M_D^2$.

In Figs.6,7 we plot the cross-sections for Y^{++} and Y^{--} productions at the LHC energy ($\sqrt{s} = 16TeV$) for different values of M_Y and M_D. We find that the crross-sections σ for Y^{++} productions are very large at LHC. For example, for $M_Y^{++} = 400GeV$, and $M_D = 200GeV$ $\sigma \simeq 10$ pb. With a projected annual luminosity of 10^5 pb^{-1}, this would correspond to about one millions Y^{++} productions. For $M_Y^{++} = M_D = 1TeV$, $\sigma \simeq$ 0.4 pb corresponding to 40,000 Y^{++} productions at LHC. The corresponding cross-sections for Y^{--} productions are somewhat smaller, but still very observable. For example, for $M_Y^{--} = 400GeV$, $M_D = 200GeV$, $\sigma \simeq 0.08$ pb, while for $M_Y = M_D = 1TeV$, $\sigma \simeq 0.0005$ pb. For Y+ productions, the cross-sections are approximately one-third of productions Y^{++}, while for Y^-, the cross-sections are the same as those for Y^{--} .

The Experimental Signatures Arising from Y^{++} and Y^{--}

In the (331) model, Y^{++} dominantly decays to l^+l^+ ($l = e, \mu, \tau$). Thus, the spectacular signal of Y^{++} production will be a pair of like sign dileptons with a peak at their invariant mass equal to the mass of the dilepton gauge bosons. Same is true for the Y^{--} productions. Below, we discuss the various kinematical possibilities

regarding M_D and M_Y, the associated multilepton signals arising from the decays of D and Y as well as the corresponding backgrounds arising from the standard model. We consider the Y^{++} and D productions and discuss the case i) $M_D > M_Y$. In this case, the decay modes of Y^{++} are l^+l^+ $(l = e, \mu, \tau)$. The decay chains of D are:

$$\begin{aligned} D &\rightarrow uY^{--} \rightarrow ul^-l^- \quad (l = e, \mu, \tau) \\ D &\rightarrow dY^- \rightarrow dl^-\nu_l \quad (l = e, \mu, \tau) \end{aligned} \tag{63}$$

Thus, the multilepton signals are either four charged leptons of the type $l_i^+l_i^+l_j^-l_j^-$ or three charge leptons of the type $l_i^+l_i^+l_j^-$ (with $l = e, \mu, \tau$ and including both i = j and i $\neq$ j possibilities). In the four charged lepton signals, there will be peaks both at the $l_i^+l_i^+$ invariant mass equaling to M_Y^{++} and the $l_i^-l_i^-$ invariant mass equaling to M_Y^{--}. For this case of $M_D > MY^{++}$; the only decay modes of Y^{++} is to l^+l^+ $(l = e, \mu, \tau)$ and the branching ratio of $Y^{++}D \rightarrow$4 charged leptons + anything is 0.5. If we consider the decays of τ to electrons or muons and consider the four charged leptons final states to be e and/or μ only, then the corresponding branching ratio is 0.24. For the three charged lepton final states, the corresponding branching ratios are the same as for the four charged lepton cases. We note that in addition to the peak at the same sign dilepton pair invariant mass distributions, these multileptons will have very high P_T since these are coming from the decay of very heavy particles (Y^{++} and D).

Now we consider the signals for $Y^{++}$and D production for the case (ii) where $M_D < M_Y$. In this case, Y^{++} can also decay to $u\overline{D}$, in addition to l^+l^+ $(l = e, \mu, \tau)$. $\overline{D}$ will decay charged leptons given in eqn.(5) via the off shell Y. Thus, for the multilepton final states, there will be peak only in one l^+l^+ pair coming from the Y^{++} decay. Branching ratios to multileptons will be essentially the same as in case (i). Again, the charged leptons will have very large P_T, compared to any standard model process. There are several source of backgrounds for the above multilepton signals coming from standard model processes. For the four charged lepton signals of the form $l_i^+l_i^-l_j^+l_j^-$ $(l = e, \mu, \tau)$, the most important background will come from

$$PP \rightarrow ZZ + anything \rightarrow l_i^+l_i^-l_j^+l_j^- + anything \tag{64}$$

At LHC, the cross section [26] times the branching ratio (with e and μ in the final states only) for the process eqn.(64) is 1.2 x 10^{-2} pb. Thus, this background is very small compared to most of the mass ranges for M_Y^{++} and D shown in figs 2. Moreover, this background is easily eliminated as the peaks in the cross sections will be in the opposite sign dilepton pairs and at M_Z compared to the peaks in the same sign dilepton pairs and at much higher mass, M_Y^{++} for the signal. Finally, these multileptons, being originated from the Z decays, will have much lower P_T and thus could also be eliminated by using suitable P_T cuts. Another important background is the two photon productions,[27] $PP \rightarrow \gamma\gamma +$ anything and the subsequent conversion of the two photons into four charged leptons. This will give rise to the combinations $l_i^+ l_i^- l_j^+ l_j^-$ ($l = e, \mu, \tau$ and including both i = j and i $\neq$ j possibilities). However, this will be a smoothly falling background without any peak in the invariant mass of two charged leptons. In addition, since these leptons originate from the photons, most of them will be produced at low P_T. Thus, using suitable P_T cuts, these backgrounds can easily be eliminated. From the four charged lepton signals, the mass ranges up to $M_Y^{++} = 1.5TeV$ and $M_D = 1.5TeV$ can be explored at the LHC, and would correspond to about 100 signal events. For the trilepton signals of the type $(l_i^+ l_i^+)$ $l_j^-(l = e, \mu, \tau)$, an important source of background is

$$PP \rightarrow ZW^{\pm} + anything \rightarrow l_i^+ l_i^- l_j^{\pm} \tag{65}$$

At LHC, σ.B[26] for the process eqn.(65) is 3.6×10^{-2} pb and is very small compared to the signal. Again, this background will have a peak at the opposite sign dilepton pairs and at M_Z, and thus can easily be eliminated. Although we have discussed in detail the signals coming from the Y^{++} productions and the associated backgrounds, the multilepton signals from Y^{--} productions and the associated backgrounds are very similar. One important difference is that Y^{--} productions cross-sections are much smaller as shown in Fig. (3). For $M_D = 200GeV$, the mass of up to 1 TeV can be explored for Y^- and will correspond to about 250 multilepton events. For $Y^{\pm}$ productions, we do not have the spectacular signal of having peaks at the same sign dilepton pairs as in the case of Y^{++} or Y^{--} productions. In this case, the

background coming from the $W^{\pm}$ pair productions becomes very important. However, for $M_D = 200$ GeV, M_Y^+ mass up to 1.5 TeV and M_Y^- up to 400 GeV can be explored at LHC using suitable $P_T$cuts. It may be mentioned that in calculating the cross sections, we have assumed that the exotic quarks, S corresponding to the 2nd family are much heavier compared to D and hence are not being produced. If S mass is comparable to the D mass, the cross -sections and threby the associated multilepton signal will increase approximately by a factor of two.

Finally, we discuss the prospect of discovering the dilepton gauge bosons in the Fermilab Tevatron ($\overline{P}P$, $\sqrt{s} = 2TeV$). For PP collider, the cross sections for Y^{++} and Y^{--} productions are the same, and are given in Table 2 (For Y^+ or Y^- productions, the corresponding cross sections are one-third of the values shown in Table 2.). For Y^{++} D (or Y^- D) productions, the cross-sections for four or three charged leptons in final states are obtained by multiplying the figures in tableII by 0.5. Thus, with the current annual luminosity of about 40 pb^{-1}, we expect 15 multilepton events (including the τ lepton) for $M_Y = M_D = 200GeV$. These multilepton events have spectacular signature, namely peaks in the same sign dilepton invariant mass distributions, and very large P_T. The backgrounds in the four charged lepton signal come from the ZZ productions and is 4×10^{-3} pb. The background for three charged lepton signals are from $ZW^{\pm}$ production and is 6×10^{-3} pb. However, in both cases, the peaks will be in the distribution of the opposite sign dilepton pairs and also at M_Z, and thus can easily be separated. P_T cut could also be used to eliminate these backgrounds. With the present luminosity, a dilepton gauge boson Y^{++} or Y^- mass of 200 GeV (for $M_D < 200$ GeV) can be explored in the Tevatron. With the projected luminosity upgrade ($L = 10^3$pb^{-1}), the mass range can be extended to 400 GeV.

TABLE II.

The values of the cross-section (in pb) for Y^{++} or Y^{--} production (same for PP collider) are shown for different values of masses of $M_D$and M_Y for the Tevatron energy (1.8 Tev)

M_Y (GeV)	M_D		
	200	300	400
200	0.673	0.183	0.051
300	0.100	0.025	0.007
400	0.018	0.005	0.001
500	0.004	0.001	0.0003

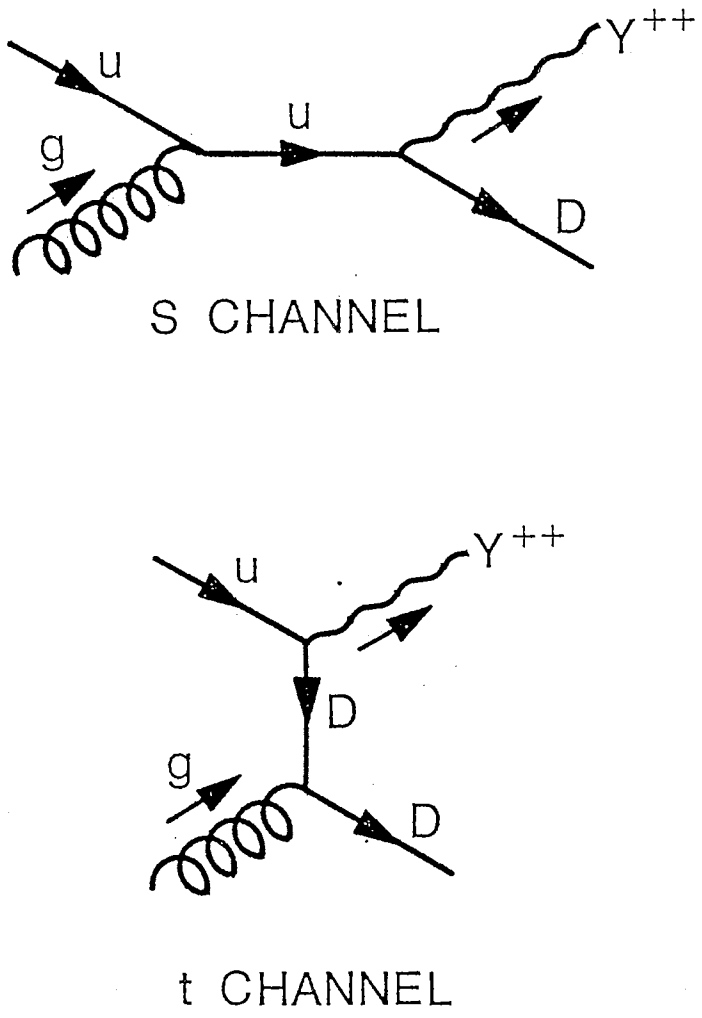

Figure 5. The Feynman diagrams for the process $u + g = Y^{++} + D$. For Y^{--} we need to change the quarks into antiquarks and vice-versa in the same diagrams. For Y^{+} production we need to change u into d and for Y^{-} we need to change the quarks into antiquarks in the same diagram.

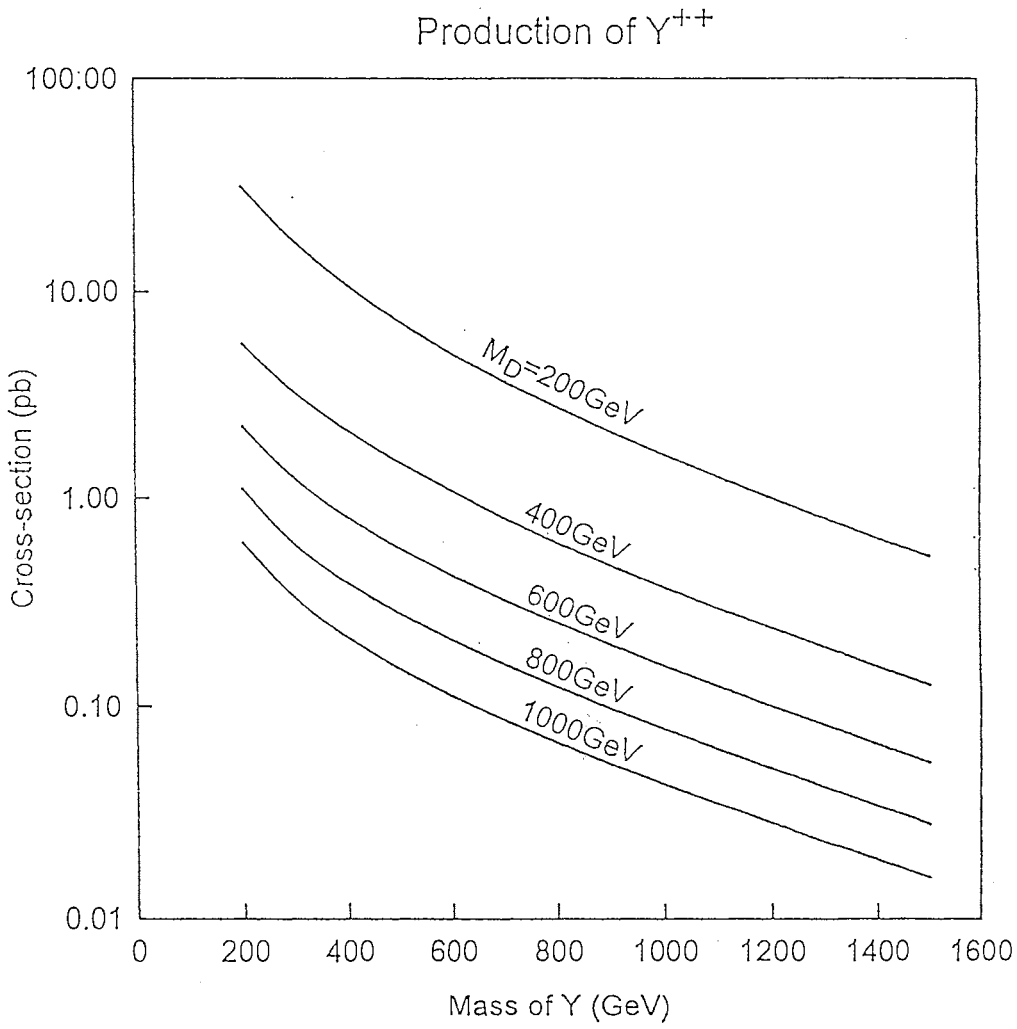

Figure 6. Cross-sections for Y^{++} production for different values of M_Y and M_D for the LHC energy ($16TeV$).

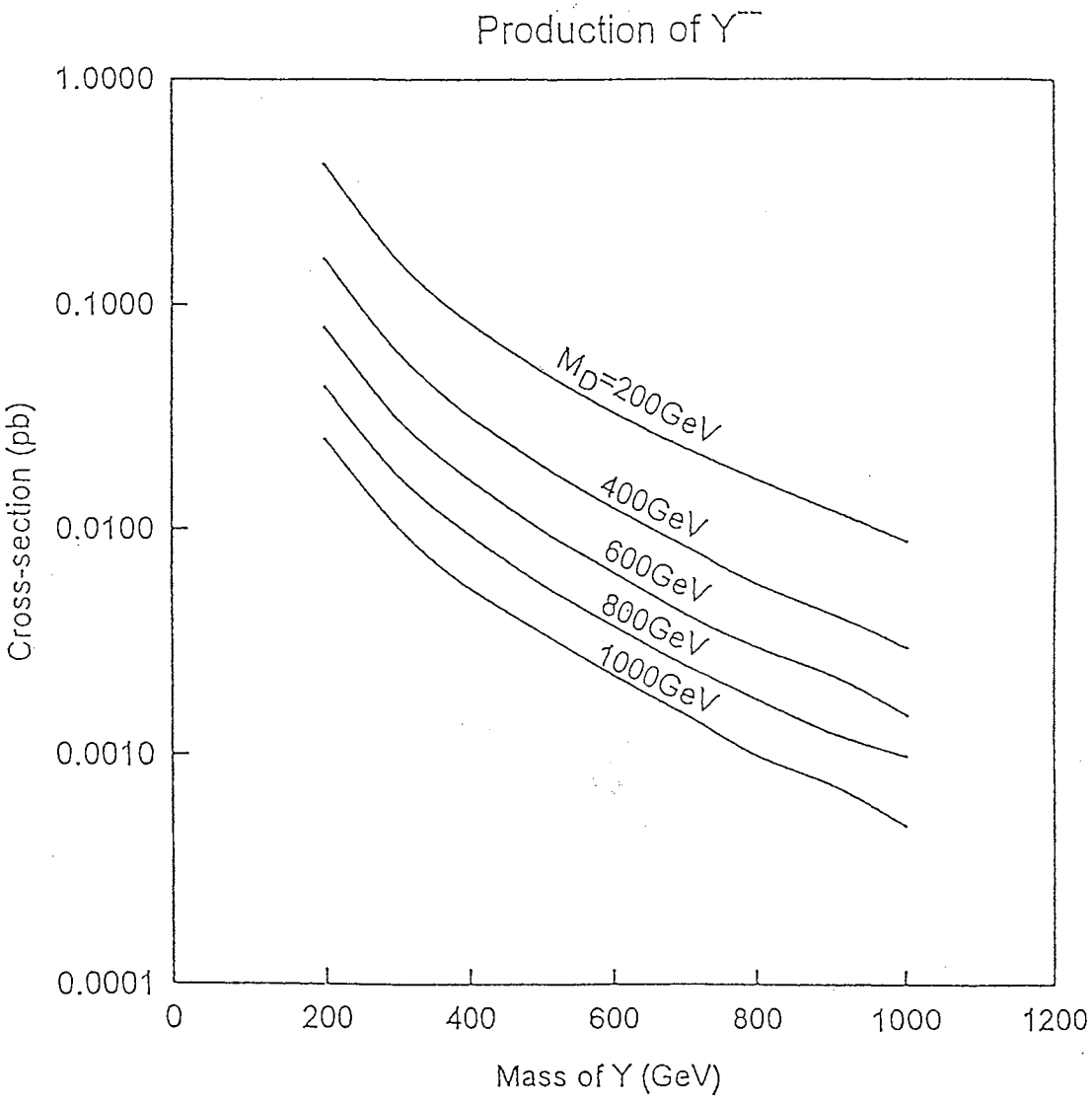

Figure 7. Cross-sections for Y^{--} production for different values of M_Y and M_D for the LHC energy ($16TeV$).

CHAPTER III

EXTENSIONS OF THE COLOR SECTOR

Introduction

The CDF collaboration at the Fermilab Tevatron has reported [28] the observation of two charged dilepton and ten single lepton+$\geq$ 3 jet events which are in excess of those expected in the Standard Model (SM) excluding $t\bar{t}$ production. A detailed analysis of seven of these events (which have at least one b-tag and a 4^{th} jet) yields the central value for top quark mass of 174 GeV and $t\bar{t}$ cross-section of 13.9 pb at the Tevatron energy ($\sqrt{s} = 1.8\ TeV$). This cross-section is about three times larger than expected in the Standard Model [29] although the error [1] is large. It is entirely possible that with larger statistics, the values of the mass and the cross-section will change to be in agreement with the SM. However, it is also possible that we are seeing the first glimpse of new physics beyond the SM at this TeV scale which is being explored directly for the first time. Several ideas have been proposed for new physics. One is to assume that the color group at high energy is bigger, namely $SU(3)_I \times SU(3)_{II}$ [10]. The color I is coupled to the first two families of fermions while the color II is coupled to the third family. This group breaks spontaneously to the usual $SU(3)_c$ at a TeV scale or below giving rise to eight massive color octet gauge bosons, called colorons. Due to mixing, these colorons couple to both the ordinary light quarks and to $t\bar{t}$. These colorons are then produced from the ordinary light $q\bar{q}$ as resonances which then decay to $t\bar{t}$, thus enhancing the $t\bar{t}$ production. The second idea assumes the multiscale models of walking technicolor[30]. The color octet technipion, η_T is produced as a resonance in the gluon gluon channel and decay dominantly to $t\bar{t}$, thus increasing the $t\bar{t}$ production to the level observed by CDF. In the third scenario, a singlet vector like charge $+\frac{2}{3}$quark is assumed with a mass comparable to the top quark

[31]. This singlet quark mixes with the top. Their production and the subsequent decay then effectively double the standard top signals [5]. Another idea proposed is that the top quark may have anomalous chromomagnetic moment type tree level coupling with the gluons [32]. A small value of the chromomagnetic moment, χ,can produce a cross- section of the level observed by the CDF Collaboration[6].

In this chapter, we discuss[33] the hadronic collider implications of the first idea above, an extended color model, $SU(3)_I \times SU(3)_{II}$, where the first two families of quarks couple to the $SU(3)_I$ whereas the third family couples to $SU(3)_{II}$, as proposed in reference (3) .We calculate the multijet and / or multilepton final state cross sections arising from production and the subsequent decay of the coloron at the Fermilab Tevatron and Large Hadron Collider(LHC) energies, and compare those with the expectations from the Standrad Model. Hill and Parke have studied the coloron production at the Fermilab Tevatron energy. At the Tevatron, the coloron is singly produced by $q\overline{q}$ annihilation. There is no contribution from gluon-gluon fusion, since there is no gluon-gluon-coloron coupling in this model. Hill and Parke showed that for the extended color symmerty breaking scale at a TeV or less, the resonant enhancement of the coloron production and their subsequent decay to $t\bar{t}$ is enough to produce the large cross-section observed by the CDF collaboration. They also study the W and top quark p_T distributions and the $t\bar{t}$ mass distributions and note that the larger p_T in this model can be used to distinguish it from the Standard Model. In this work, we proceed further by looking at the decay products of the Ws and making some simple visiblity cuts to test the extent to which the p_T distributions as they would be observed, are really different. However, the main part of our work is to study the implications of the model at the LHC energy ($pp, \sqrt{s} = 14TeV$). Here, the colorons can be pair-produced via gluon-gluon fusion. Each coloron decays to a $t\bar{t}$ or $b\bar{b}$ pair. If we look at the tops, we get two top quarks and two top antiquarks whose decays give rise to four W bosons in the final state. The cross-sections for these four W final states are much larger than those in the Standard model. This anomalous W productions will be very clean signal for physics beyond the Standard Model at high energy hadronic colliders such as LHC. We also calculate the branching ratios for the

various multijet and/or multilepton final state arising from the subsequent decays of these final state Ws.

Formalism For The $SU(3)_I \times SU(3)_{II}$ Color Model

The gauge part of the of the $SU(3)_I \times SU(3)_{II}$ extended color model is

$$-L_{gauge} = \frac{1}{4} F_{I\mu\nu a} F_{Ia}^{\mu\nu} + \frac{1}{4} F_{II\mu\nu a} F_{IIa}^{\mu\nu} \tag{66}$$

where

$$F_{I\mu\nu a} = \partial_\mu A_{I\nu a} - \partial_\nu A_{I\mu a} - h_1 f_{abc} A_{I_{\mu b}} A_{I\nu c}$$

and similarly for $F_{II\mu\nu a}$ with $h_1$replaced by h_2.The expressions h_1 and h_2 represent the two color gauge coupling constants. The $SU(3)_I \times SU(3)_{II}$ symmetry is broken spontaneously to the usual $SU(3)_c$ at some scale M at or below a TeV. This is achieved by using a Higgs field, Φ which transform like $(1,3,\bar{3})$ under $(SU(2)_L, SU(3)_I, SU(3)_{II})$ with VEV=diag.(M,M,M). At low energy, we are left with eight massless gluons ($A_{\mu a}$) and eight massive colorons ($B_{\mu a}$) defined as

$$A_I = A\cos\theta - B\sin\theta$$

$$A_{II} = A\sin\theta + B\cos\theta \tag{67}$$

where θ is the mixing angle, and

$$g_3 = h_1\cos\theta = h_2\sin\theta\cdot \tag{68}$$

The mass of the coloron is

$$M_B = \left(\frac{2g_3}{\sin 2\theta}\right) M\cdot \tag{69}$$

In terms of the gluon (A) and the coloron field (B), we can write the gauge part of the interaction schematically as

$$-L_{gauge} = \frac{1}{2}g_3\left[A^3 + 3AB^2 + 2\cot 2\theta B^3\right] + \frac{1}{4}g_3^2[A^4 + 6A^2B^2 + 4\left(2\cot 2\theta\right)AB^3 + \left(\tan^2\theta + \cot^2\theta - 1\right)B^4] \quad (70)$$

In Eq.(70), A^3 and A^4 represent schematically the usual three and four point gauge interactions, namely,

$$A^3 \equiv f_{abc}(\partial_\mu A_{\nu a} - \partial_\nu A_{\mu a})A^{\mu b}A^{\nu c}$$

and

$$A^4 = f_{abc}f_{ade}A_{\mu b}A_{\nu c}A_d^\mu A_e^\nu \quad (71)$$

We see from Eq.(70) that a single coloron does not couple to two or three gluons. Thus, a single coloron or a coloron in association with a gluon can not be produced in hadronic colliders from gluon-gluon fusion.

The fermion representations under $(SU(2)_L, SU(3)_I, SU(3)_{II})$ are

$(u,d)_L, (c,s)_L \to (2,3,1)$; $(u_R, d_R, c_R, s_R) \to (1,3,1)$

$(\nu_e, e)_L, (\nu_\mu, \mu), (\nu_\tau, \tau)_L \to (2,1,1)$; $(e_R, \mu_R, \tau_R, \nu_{iR}) \to (1,1,1)$

$$(t,b)_L \to (2,1,3); (t_R, b_R) \to (1,1,3). \quad (72)$$

it needs to be noted that the first two families of quarks couple to the color I while the third family of quarks couples to color II. This assignment is anomaly free. With the above assignment, the interactions of all the quark with the gluons are same as in the usual QCD. The interactions of the colorons are given by

$$-L_{coloron} = g_3\left[z_1\sum_i \overline{q_i}\gamma^\mu\frac{\lambda^a}{2}q_i + z_2\left(\bar{t}\gamma^\mu\frac{\lambda^a}{2}t + \bar{b}\gamma^\mu\frac{\lambda^a}{2}b\right)\right]B_{\mu a} \quad (73)$$

where the sum i is over u, d, s and c quarks.

$$z_1 = -\tan\theta, \qquad z_2 = \cot\theta \quad (74)$$

so that $z_1 z_2 = -1$;

Results For Fermilab Tevatron

In this section, we discuss $t\bar{t}$ production and the resulting multijet and/or multilepton final states at the $\bar{p}p$ collider at the Fermilab Tevatron, $\sqrt{s} = 1.8$ TeV. The dominant subprocess is the annihilation of ordinary $q\bar{q}$ pair to produce $t\bar{t}$ via coloron exchange in the s-channel, in addition to the usual standard model processes. (The contribution of gg subprocess producing two colorons is either kinematically not allowed or negligible). The total cross-sections depends on the coloron mass as well as the coloron width. We use Eq. (8) for our calculations, and following Hill and Parke, present our results for the coloron model, $z_1z_2 = -1$ (Eq. 9), as well as for another model which is like the coloron model except the value of $z_1z_2 = +1$. [The value of $z_1z_2 = +1$ can be obtained in a color singlet vector resonance model with an extra U(1) [34]]. For parton distributions, we use those produced by the CTEQ collaboration[35].

Hill and Parke note that in their models, the top quark and the W boson have larger p_T than in the Standard Model and that this could be used to distinguish these models from the standard model with only a relatively small number of top events. Here,we proceed slightly further by looking at the decay products of the Ws and making some simple visibility cuts.

In particular, we keep the matrix element for top decay into $bl\overline{\nu}$ or $bq\overline{q}$ so as to include the coherent polarization sum of the Ws. We then combine the quarks into jets by requiring that final state quarks be in the same jet if their angular separation is less than $\Delta R = 0.5$ with the standard definition of ΔR. We next require that jets and the charged leptons from the Ws be visible by requiring that their p_T be larger than some $p_T^{\min}$ and that their rapidity y be less than some y^{max}. We also require that these leptons be separated from the jets, and from each other, if there is more than one, by $\Delta R \geq 0.5$.

Using these criteria, we find the branching ratios for n jets and m charged leptons where n=0,1,2,3,4,5,6 and m=0,1,2. We do this for the standard model and for the following four models of Hill and Parke: (a) $z_1z_2 = -1$, $M_B = 400GeV$, $\Gamma_B =$

$0.6M_B$; $(b)z_1z_2 == +1, M_B = 600GeV$, $\Gamma_B = 0.2M_B$; $(c)z_1z_2 = -1$, $M_B = 600GeV$, $\Gamma_B = 0.5M_B$ and (d) $z_1z_2 = +1$, $M_B = 400$, $\Gamma_B = M_B$.

As can be seen from Fig.1, each of these four models have a total cross-section near 14 pb. Table III gives the branching ratios if y^{max} is 1.5 and p_T^{min} is 35 GeV. Clearly, there is very little difference between these models and the standard model (which is the top number in each set of five) so far as BR's are concerned. Table IV gives the same cases for $p_T^{min} = 50$ GeV. Here, the new models do show some p_T behavior (except for model (a)) but the branching ratios for the interesting topologies, for example, four jets and one lepton for are quite small. If the detector efficiency is 10% and we have 1000 pb^{-1} of integrated luminosity then the standard model gives 2.4 events of 4 jet, 1 lepton type, while the new models give 4.2 to 23 events. Of course, a large part of the extra events in the new models is still just the larger cross-section 14 pb vs 5 pb for the standard model.

We have also investigated other values of M_B and Γ_B/M_B and found similar results. For $p_T^{min} = 35GeV$, the additional p_T inherent in these models is of only modest help in increasing the branching ratios of the interesting topologies. For $p_T^{min} = 50GeV$ the additional p_T is a big help but the branching ratios themselves are quite small.

It may be noted that the charged leptons we talk about, imply electrons or muons. We include the tau lepton by assuming it decays immmediately after production into a muon or electron plus neutrinos (35.5% of the time) or into a quark pair plus a neutrino (64.5% of the time). Thus the visible final states of a W decay through a tau have the same particle content as other W decays: an electron, a muon, or a pair of quarks. The possible energies of the visible particles are, undoubtedly, different if the decay is through a tau, and that has been included.

Coloron Signal at LHC Energy

In this section, we discuss the coloron pair productions in hadronic collisions in the spontaneously broken $SU(3)_I \times SU(3)_{II}$ extended color model. We consider only the case where each coloron decays to top quarks, $t\bar{t}$. Decays of these t(or $\bar{t}$)

TABLE III.

Branching ratios for the various multijet and multilepton final states with each jet and charged lepton e, μ having $p_T > 35$ GeV and with other cuts as discussed. The results are for the Tevatron energy, $\sqrt{s}$=18 TeV. SM stands for Standard model a, b, c and d are the four different models discussed in the text

jets \ leptons		0	1	2
	(SM)	1.81E-3	2.32E-3	9.09E-4
	(a)	2.17E-3	2.14E-3	7.59E-4
0	(b)	2.00E-3	2.17E-3	1.27 E-3
	(c)	1.80E-3	2.20E-3	1.01 E-3
	(d)	1.95E-3	2.15E-3	9.93 E-3
		0.0251	0.0245	5.93E-3
		0.0249	0.0259	5.48E-3
1		0.0191	0.0240	7.89E-3
		0.0231	0.0256	6.45E-3
		0.0229	0.0253	6.45E-3
		0.115	0.0825	9.00E-3
		0.121	0.0810	8.53E-3
2		0.0874	0.0786	0.0124
		0.107	0.0819	9.92E-3
		0.106	0.0823	0.0104
		0.236	0.0897	
		0.240	0.0847	
3		0.188	0.106	
		0.225	0.0938	
		0.220	0.0942	
		0.239	0.0298	
		0.239	0.0270	
4		0.230	0.0473	
		0.238	0.0334	
		0.239	0.0361	
		0.117		
		0.110		
5		0.152		σ:4.810 $\pm$ 0.009 pb SM
		0.126		:13.93 $\pm$ 0.03 pb (a)
		0.128		:13.49 $\pm$ 0.04 pb (b)
				:13.52 $\pm$ 0.02 pb (c)
		0.0209		:13.89 $\pm$ 0.03 pb (d)
		0.0177		
6		0.0388		
		0.0241		
		0.0263		

TABLE IV.

Same as in table III except for $p_T > 50$ GeV.

jets \ leptons		0	1	2
	(SM)	0.0155	6.81E-3	1.36E-4
	(a)	0.0188	7.30E-3	1.31E-4
0	(b)	0.0107	5.70E-3	1.84 E-3
	(c)	0.0148	6.66E-3	1.53 E-3
	(d)	0.0137	6.85E-3	1.57 E-3
		0.105	0.0430	3.48E-3
		0.109	0.0455	3.04E-3
1		0.0602	0.0395	6.04E-3
		0.0927	0.0428	3.98E-3
		0.0876	0.0437	4.32E-3
		0.270	0.0670	2.50E-3
		0.295	0.0631	1.87E-3
2		0.177	0.0795	5.73E-3
		0.257	0.0696	2.85E-3
		0.250	0.0720	3.12E-3
		0.280	0.0370	
		0.290	0.0304	
3		0.258	0.0684	
		0.283	0.0409	
		0.278	0.0447	
		0.130	4.58E-3	
		0.121	2.48E-3	
4		0.197	0.0161	
		0.141	5.97E-3	
		0.150	6.70E-3	
		0.0262		
		0.0176		
5		0.0722		
		0.0320		
		0.0355		
		2.29E-3		
		7.31E-3		
6		9.62E-3		
		3.14E-3		
		3.49E-3		

to a W give rise to four W bosons in the final state. The cross-section for these four W productions is much larger than that expected in the Standard model. This anomalous W productions will be a very clean signal for physics beyond the Standard Model.

The dominant contribution to the coloron pair production at the LHC enengy comes from the subprocess

$$g + g \rightarrow B + B \tag{75}$$

The corresponding Feyman diagrams obtained from Eq.(70) are shown in Fig. 2. The contribution of the other subprocess $q + \overline{q} \rightarrow B + B$ (Eq. 8) is very small at the LHC energy because of the low $q\overline{q}$ luminosity.

The differential cross-section for the subprocess Eq.(75) is obtained to be

$$\frac{d\hat{\sigma}}{dz} = \frac{9\pi\alpha_s^2}{512\hat{s}}\beta F(\varepsilon, z) \tag{76}$$

where

$$\begin{aligned} F(\epsilon, z) = \; & [\tfrac{1}{(1+\beta z)^2}(256 + \tfrac{48}{\epsilon^2}) \\ & + \tfrac{1}{(1+\beta z)}(-128 - \tfrac{96}{\epsilon} + \tfrac{24}{\epsilon^2}) \\ & + (z \rightarrow -z)] \\ & + 200 + 24\beta^2 z^2 + \tfrac{48}{\epsilon} \end{aligned} \tag{77}$$

Here, $\hat{s}$ is the total center of mass (CM) energy squared for the subprocess, z is the cosine of the CM angle, M_B is the mass of the coloron, B, α_s is the QCD coupling constant squared over 4π, and

$$\epsilon \equiv \frac{\hat{s}}{4M_B^2}, \qquad \beta \equiv \left(1 - \frac{1}{\epsilon}\right)^{\frac{1}{2}} \tag{78}$$

From Eq. (76), we obtain the total subprocess cross-section to be

$$\hat{\sigma} = \tfrac{9\pi\alpha_s^2}{512\hat{s}}\beta\left[\left(1024\epsilon + 416 + \tfrac{272}{\epsilon}\right) - \left(256 + \tfrac{192}{\epsilon} - \tfrac{48}{\epsilon^2}\right)\tfrac{1}{\beta}\ln\tfrac{1+\beta}{1-\beta}\right] \tag{79}$$

The total cross section for the process

$$p + \overline{p} \rightarrow B + B + anything \tag{80}$$

is obtained by folding in the gluon distributions with the above cross section. We have used the distribution produced by the CTEQ collaboration [8] evaluated at $Q^2 = M_B^2$.

Multijet-Multilepton Final States from Coloron Pair Decays

Using the production cross-section above, and assuming the branching ratio for each final states of W decay to be $\frac{1}{9}$, we find the branching ratio for n jets and m charged leptons where n = 0,$\cdots$,12 and m = 0,$\cdots$,4. These results depend on the mass of the coloron, the visibility cuts, and the mixing with light quarks (z_1 and z_2 in (8) above). To isolate the combinations which can not be produced in lowest order of the SM we consider only the $t\bar{t}\ t\bar{t}$ final state.

As in the Fermilab results above, we combine the quarks into jets using the condition that a quark belongs in an adjacent jet if the angular separation between them is less than ΔR which we take to be 0.5. Once the jets are formed, their transverse momentum is required to be larger than 30 GeV and their rapidity less than 2. For the leptons (electron or muon), we require a tranverse momentum of 20 GeV and a maximum rapidity of 2.5. The leptons must be separated from the jets, and from each other by $\triangle R$ which is also taken to be 0.5. Thus, for example, if each of the two leptons satisfy the transverse momentum and rapidity cuts but have $\triangle R$ less than 0.5, then they are counted as only one lepton.

If the final state of a W decay is a tau lepton, then we assume the tau has decayed and use its decay products in forming jets and applying the visibility cuts. In other words, in case of a tau, we proceed one level further in the decay chain to find the particles we treat as the final state.

We keep a coherent sum over the polarizations of the Ws from the top decays but not for the Ws in the tau decays. We do not keep a coherent spin sum for the tops.

Our results are given in Tables V-[?] for a coloron mass of 400, 600, and 800 GeV. We give results only for the branching ratios for events with more jets or leptons than can be directly produced in the SM, or by other final states of the colorons, $t\bar{t}$ $b\bar{b}$ for example. To include mixing with the lighter quarks each branching ratio should be miltiplied by

$$\left[\frac{z_2^2 I}{4z_1^2 + z_2^2 + z_2^2 I}\right]^2$$

where I is given by

$$I = \left(1 + 2\frac{m_t^2}{M_B^2}\right)\left(1 - 4\frac{m_t^2}{M_B^2}\right)^{\frac{1}{2}}$$

These branching ratios are rather small. Fortunately the production cross sections are large so that the actual number of events with these topologies can be large.

TABLE V.

Branching ratios for the various multijet and multilepton (e or μ) final states at the LHC energy, $\sqrt{s}$ =14 TeV for the coloron model with coloron mass M_B= 400 GeV. The cuts are $\left(p_T^{jets}\right)_{\min} = 30\ GeV$, $\left(p_T^{leptons}\right)_{\min} = 20\ GeV$,$y_{jet} \leq 2.0$, $y_{lepton} \leq 2.5$, and $\Delta R = 0.5$ everywhere.

jets \ leptons	0	1	2	3	4
0				1.18E-5	1.80E-6
1				1.76E-4	3.55E-5
2				1.15E-5	1.67E-4
3				3.30E-3	3.50E-4
4				5.05E-3	2.43E-4
5			0.0326	3.86E-3	
6			0.0258	1.04E-3	
7		0.0770	0.0103		
8		0.0391	1.69E-3		
9	0.0589	0.0106			
10	0.0192	1.11E-3		$\sigma = 758 \pm 2$pb	
11	4.01E-3				
12	3.51E-4				

TABLE VI.

Same as in tableV, except for M_B= 600 GeV.

jets \ leptons	0	1	2	3	4
0				4.75E-6	1.37E-6
1				9.65E-5	2.45E-5
2				7.94E-5	1.66E-4
3				3.13E-3	4.29E-4
4				6.03E-3	3.65E-4
5			0.0347	5.40E-3	
6			0.0335	1.86E-3	
7		0.0942	0.0173		
8		0.0607	3.73E-3		
9	0.0792	0.0207			
10	0.0350	3.22E-3		σ=67.32 $\pm$ 0.16pb	
11	9.75E-3				
12	1.09E-3				

TABLE VII.

Same as in tableV, except for M_B= 800 GeV.

jets \ leptons	0	1	2	3	4
0				1.71E-6	7.62E-7
1				6.02E-5	1.70E-5
2				5.92E-5	1.29E-4
3				2.76E-3	3.61E-4
4				5.51E-3	3.23E-4
5			0.0334	4.76E-3	
6			0.0302	1.55E-3	
7		0.0879	0.0142		
8		0.0607	3.73E-3		
9	0.0687	0.016			
10	0.0287	2.29E-3		σ=9.448 $\pm$ 0.024pb	
11	6.71E-3				
12	8.79E-3				

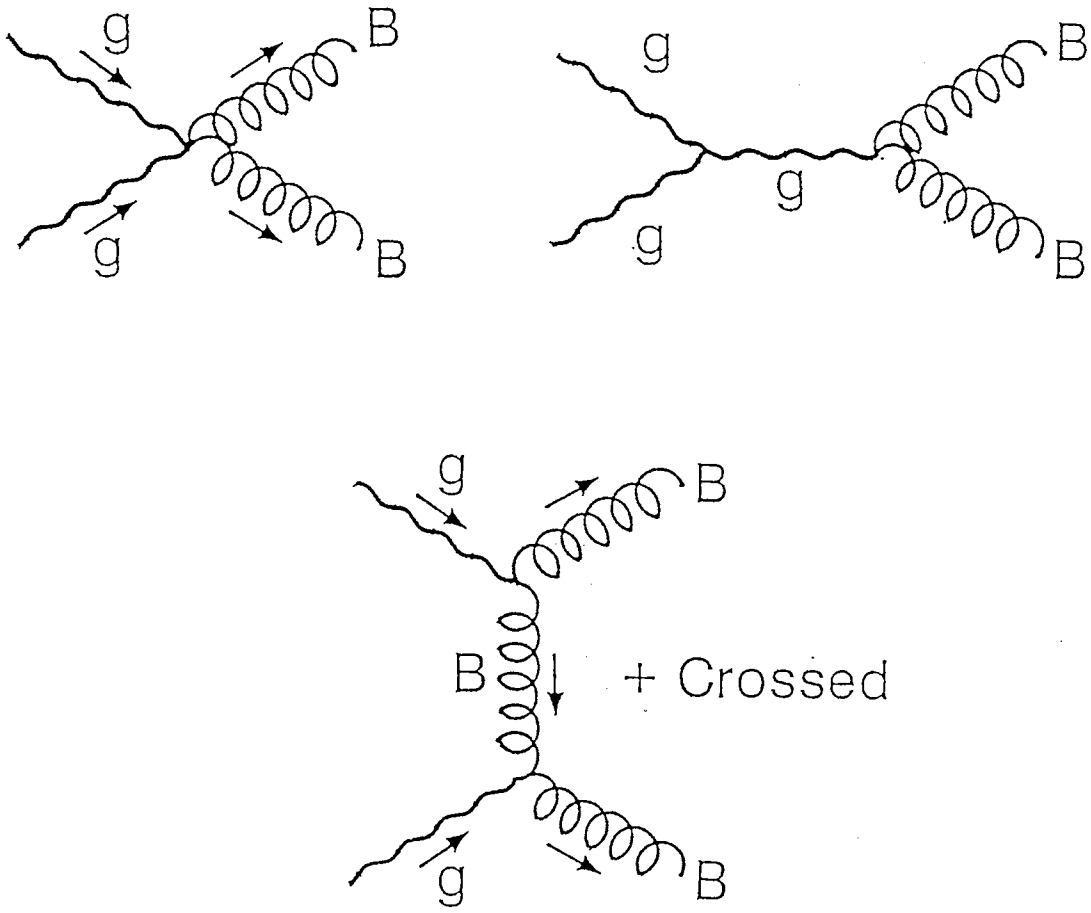

Figure 8. Feynman diagrams for the process gluon+gluon → coloron+coloron.

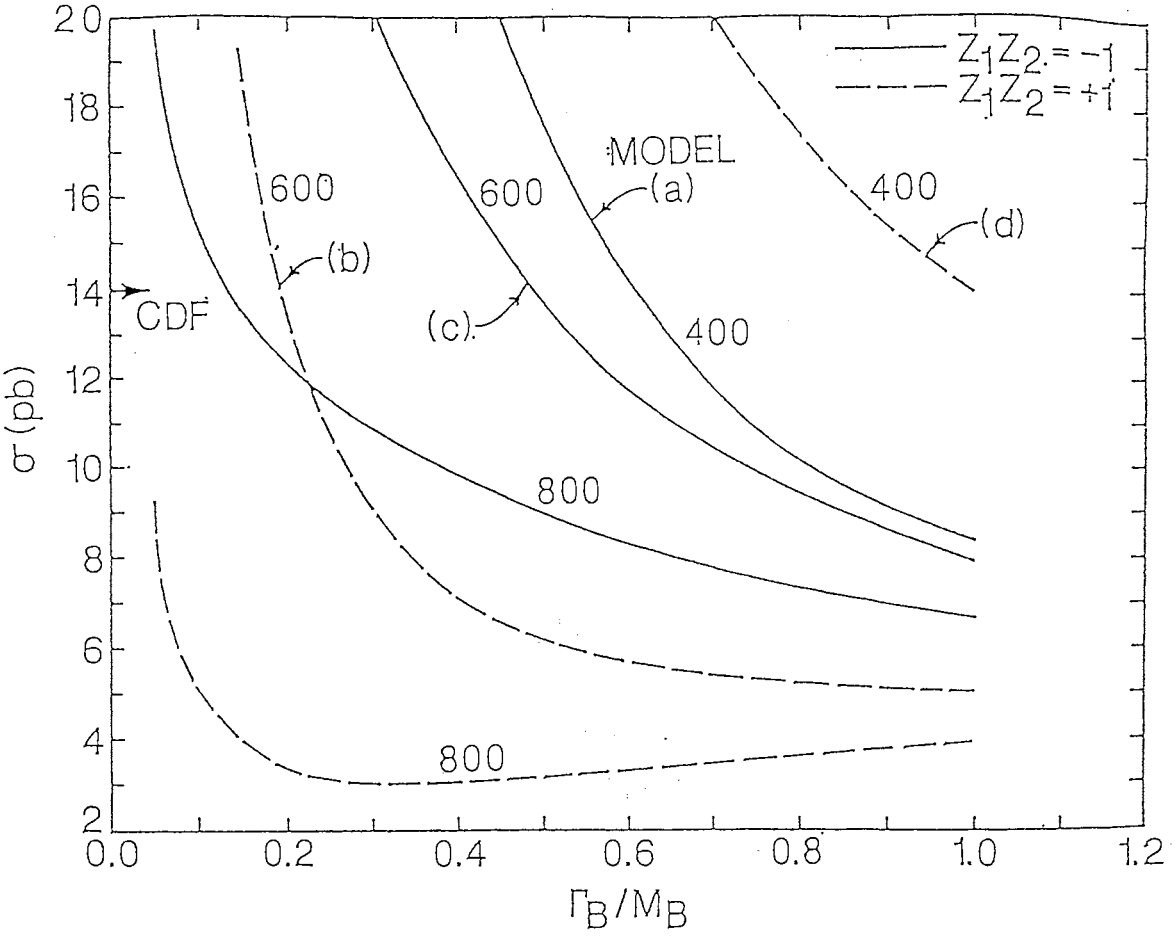

Figure 9. Cross sections (in pb) for the $t\bar{t}$ pair productions at the Tevatron. $M_B$and Γ_B are the mass and the width of the coloron. The solid curves are for z_1z_2 = -1 white the dotted curves are $z_1z_2 = +1$ as discussed in the text. The numbers indicated with the curves are the coloron masses in GeV. The four models discussed in the text are indicated by (a), (b),(c) and (d). The experimental value of the cross section, as measured by CDF collaboration, is shown by the arrow.

CHAPTER IV

EXTENSION TO SUPERSYMMETRY

Introduction

The original motivation of applying Supersymmetry to particle physics was to solve the gauge hierarchy problem that has arisen in the grand unification program. Recent LEP data shows that only in the supersymmetric version of the theory, one can realize the proper unification. So, if Supersymmetry exists with the superparticles around the 100 GeV -1 TeV scale, then it is possible to observe its effect through b or μ . In this chapter, we try to see the effect of Supersymmetry through b decays.

The flavor changing decay $b \to s\gamma$ is often an important test of new physics because it is rapid enough to be experimentally observable although it appears first at the one loop level in the standard model (SM), thus allowing new physics to add sizeable corrections to it. For example, the decay is useful to limit parameter space in the minimal supersymmetric standard model (MSSM) [36–47]. This is an especially useful tool if certain constraints have already been placed on the MSSM. Since the decay vanishes in the limit of unbroken supersymmetry, the relevant constraints pertain to the terms in the Lagrangian that softly break supersymmetry (SUSY). The general soft SUSY breaking scalar interactions for squarks and sleptons in the MSSM are of the following form:

$$\begin{aligned} V_{\text{soft}} &= Q(\mathbf{A}_U\lambda_U)U^cH_2 + Q(\mathbf{A}_D\lambda_D)D^cH_1 + \text{h.c.} \\ &+ Q^\dagger\mathbf{m}_Q^2Q + U^{c\dagger}\mathbf{m}_U^2U^c + D^{c\dagger}\mathbf{m}_D^2 + L^\dagger\mathbf{m}_L^2L + E^{c\dagger}\mathbf{m}_E^2E^c\,, \end{aligned} \tag{81}$$

where Q and L are squark and slepton doublets and U^c, D^c, and E^c are squark and slepton singlets. It is most frequently assumed that soft breaking operators are induced by supergravity, and that these operators have a universal form which is

generation symmetric and CP conserving. Usually, this assumption is coupled with that of grand unification to provide further constraints on the model's parameters. For purposes of simplicity, the universal boundary condition is traditionally taken at the grand unification scale, even though the soft-breaking operators would be present up to near the Planck scale. The universal soft SUSY-breaking boundary condition is described by the following parameters: the scalar mass m_0, the gaugino mass $m_{1/2}$, and the trilinear and bilinear scalar coupling parameters A and B, respectively.

Grand unification and $b \to s\gamma$

Despite convention, some recent papers [48–51] have demonstrated important implications of taking the boundary conditions at the Planck scale M_P and evolving them down to the scale M_G where grand unification is broken. The important difference between taking the universal boundary condition at the Planck scale and the GUT scale is because of the top quark mass is known to be large ($\sim$ 174GeV) and grand unification causes some fields to feel the effects of the top coupling by unifying them into the same multiplet with the top. For example, in SU(5) grand unification, Q, U^c, and E^c together become transformed as the **10**-representation. Taking the universal boundary condition at the GUT scale ignores the fact that the soft-breaking parameters run above the GUT scale. One may at first think that any effect of grand unification would be suppressed by powers of $1/M_G$, but it has been demonstrated that such effects rather depend on $\ln(M_P/M_G)$ [52]. One surprising result, which is given in refs. [49,51], is that the predicted rate for the lepton flavor violating decay $\mu \to e\gamma$ may be only one order of magnitude beneath current experimental limits. This is found even in SU(5) grand unification, where only neutralinos are available to mediate the decay at the one-loop order. However because of the the soft-breaking masses being assumed to be flavor blind and the unitarity of the CKM mixing matrix, one might naively expect the partial width to vanish. But this does not happen because operators with strength of the top coupling cause the third generation scalar fields contained in the **10**-representation, in SU(5), to be considerably lighter than the corresponding fields of the other two generations [49]. Below the grand unification

scale, the only squarks effected by the top Yukawa coupling are the top singlet and the third generation $SU(2)_L$ squark doublet. We would apply these facts to demonstrate that in some of the same regions of parameter space where chargino corrections are important, one might also expect sizeable corrections from gluinos. For some parameter space, not only is the contribution from the gluinos important, but in fact it is also greater than that of the charginos. The fact that the top squark soft breaking masses are lighter when the universal boundary condition is taken at the Planck scale rather than the grand unification scale is, of course, likewise felt by the wino and higgsino-wino mediated decays.

The standard model amplitude for $b \to s\gamma$ has been derived in refs. [53,54], and expressions for the additional MSSM amplitudes have been derived in refs. [37–39], with ref. [37] containing the first and most complete derivation. The QCD corrected version [39,55,56] of the partial width is given as a ratio to the inclusive semi-leptonic decay width in the following form:

$$\frac{\Gamma(b \to s\gamma)}{\Gamma(b \to ce\nu)} = \frac{6\alpha}{\pi\rho\lambda} \frac{|V_{ts}^* V_{tb}|^2}{|V_{cb}|^2} |c_7(m_b)|^2 , \tag{82}$$

where α is the electromagnetic coupling, $\rho = 1 - 8r^2 + 8r^6 - r^8 - 24r^4 \ln r$ with $r = m_c/m_b = 0.316 \pm 0.013$ is the phase-space factor, and $\lambda = 1 - (2/3\pi) f(r) \alpha_s(m_b)$ with $f(r) = 2.41$ is the QCD correction factor. The ratio of the CKM matrix entries, for which we will use the experimental mid-value, is $|V_{ts}^* V_{tb}|^2 / |V_{cb}|^2 = 0.95 \pm 0.04$. The QCD corrected amplitude $c_7(m_b)$ is given as

$$c_7(m_b) = \eta^{16/23} \left[c_7(M_W) - \frac{8}{3} c_8(M_W) \left[1 - \eta^{-2/23} \right] \right] + \sum_{i=1}^{8} a_i \eta^{b_i} , \tag{83}$$

with a_i and b_i being given in ref. [56], $\eta = \alpha_s(M_W)/\alpha_s(m_b)$, for which we will use $\eta = 0.548$, and $\Gamma(b \to ce\nu) = 0.107$. The terms $c_7(M_W)$ and $c_8(M_W)$ are respectively A_γ, the amplitude for $b \to s\gamma$ evaluated at the scale M_W and divided by the factor $A_\gamma^0 \equiv 2G_F \sqrt{\alpha/8\pi^3} V_{ts}^* V_{tb} m_b$ and A_g, the amplitude for $b \to sg$ divided by the factor $A_\gamma^0 \sqrt{\alpha_s/\alpha}$. The effective interactions for $b \to s\gamma$ and $b \to sg$ are given by

$$L_{\text{eff}} = \frac{A_\gamma^0}{2} \left(A_\gamma \bar{s} \sigma^{\mu\nu} P_R b F_{\mu\nu} + A_g \bar{s} \sigma^{\mu\nu} P_R b G_{\mu\nu} \right) + \text{h.c.} . \tag{84}$$

Previous calculations of $b \to s\gamma$ in the MSSM have routinely either ignored the contributions mediated by gluinos [39–44,46] or found them to be less important [36–38,45,47] than we do. This is primarily because, unlike the previous treatments, we are intersted in taking the soft breaking universal boundary condition at the Planck scale which enhances the gluino contribution over taking the universal boundary condition at the GUT breaking scale, M_G. However, even when we take the boundary condition at M_G, we will find the gluino mediated contribution to be greater than one would find according to the methods of the previous calculations that examined the gluino mediated contribution. This is due to the fact that unlike in those references, we include the QCD corrections from the O_8 operator in running c_7 from the M_W scale down to m_b scale. This is as is done in, for example, refs. [39–41,46,55,56]. In other words, the previous studies which included gluino mediated decays used the approximation $c_8(M_W) = 0$ in Eq. (84) Despite that, as observed in ref. [36], the gluino contribution to $b \to sg$ can be significant due to the fact that the gluon can couple to the gluino in the gluino-squark loop. In calculating $c_7(M_W)$ and $c_8(M_W)$, we will however use the conventional approximation of taking the complete MSSM to be the correct effective field theory all the way from the scale M_G down to M_W.

As previously stated, normally A_γ is taken to be approximately the sum of A_γ^W, $A_\gamma^{H^-}$, and $A_\gamma^{\tilde{\chi}^-}$. In such a case, the charged Higgs contribution adds constructively to the SM amplitude. On the other hand, the chargino amplitude may combine either constructively or destructively with the other two, and in some cases may even cancel the charged Higgs amplitude. Even though the squarks strongly couple to the gluino, the contribution from the gluino mediated diagrams are considered negligible because the three generations of down squarks $\tilde{d}_{iL}$ belonging to $\tilde{Q}_{Li}$ are conventionally assumed to have degenerate soft-breaking masses at the GUT breaking scale. However, the mass parameter $m^2_{\tilde{Q}_{3L}}$ is reduced by a small amount relative to $m^2_{\tilde{Q}_{iL}}$ for the first two generations in running the mass parameters down from the GUT scale, and b-squark mass matrix has off-diagonal entries proportional to m_b as given in the following

equation:

$$m_{\tilde{b}}^2 = \begin{pmatrix} m_{\tilde{Q}_{L3}}^2 + m_b^2 - \frac{1}{6}(2M_W^2 + M_Z^2)\cos 2\beta & m_b(A_b + \mu \tan\beta) \\ m_b(A_b + \mu \tan\beta) & m_{\tilde{b}_R}^2 + m_b^2 + \frac{1}{3}(M_W^2 - M_Z^2)\cos 2\beta \end{pmatrix}, \quad (85)$$

where $\tan\beta = v_2/v_1$ is the ratio of Higgs vacuum expectation values and μ is the coefficient of the Higgs superpotential interaction $\mu H_1 H_2$. These two effects make the b-squark eigenvalues somewhat different from the down squark masses of the other two generations. However, the total effect is insignificant compared to the mass splitting that takes place in the stop sector due to the size of the top quark mass. (See, for example, Fig. 8 in ref. [57]) For this reason, and because the chargino contribution includes an often highly significant higgsino mediated decay, the chargino contribution to $b \to s\gamma$ is found to be very important for some regions of parameter space, while the gluino and neutralino contributions are conventionally either found or assumed to be of little signifigance when the universal boundary condition is taken at the scale M_G.

Calculation of $b \to s\gamma$ Amplitude

Now, we will perform[58] the calculation with the universal boundary condition taken at the Planck scale and run the soft breaking parameters from there down to the weak scale. In the following discussion, we will use the one loop renormalization group equations for the gauge couplings, top Yukawa coupling, and soft breaking masses (See refs. [36,48,59]). We will also use the exact analytic solutions, in the form derived in ref. [51], to these one loop equations. We will use the conventions for the sparticle mass matrices and the trilinear coupling parameter A_i as found in ref. [SUSY]. ($A_i \to -A_i$ in the RGEs and RGE solutions of ref. [51].) We will use $\alpha_s(M_Z) = 0.12$. For the purpose of illustration, we will consider the specific case where the Planck scale trilinear scalar coupling $A_0 = 0$, $\tan\beta = 1.5$, $\lambda_t(M_G) = 1.4$, and the grand unification model is the minimal SUSY SU(5) model. If $\lambda_t(M_G)$ is reduced significantly, then also would be the effects that we are discussing. For our chosen values of the top coupling and $\tan\beta$, the top quark pole mass is about 168 GeV. For larger $\tan\beta$, the gluino and neutralino contribution would be greatly increased [38].

However, at the same time, this would tend to occur for sparticle masses where the chargino contribution to $b \to s\gamma$ is large enough to rule out the region of parameter space.

Since the off diagonal terms in the b-squark mass matrix are much smaller than the diagonal ones and give relatively only a small contribution to the mass splitting between the b-squark mass eigenstates, we choose for simplicity to take the b-squark mass eigenstates to be the soft breaking masses. (See ref. [50].) The two types of diagrams that contribute to $b \to s\gamma$ and $b \to sg$ in SU(5) with $\tilde{d}_{iL}$ running in the internal loop are shown in Fig. 10. The internal fermion line represents either a gaugino or a neutralino propagator. To derive the contributions to A_γ or A_g, one must sum the graphs with an external photon or gluon, respectively, attached in all possible ways. It is possible and simplest to work in a basis in which $\lambda_{\mathbf{U}}$, the soft breaking squark masses and the trilinear couplings A are always diagonal in generation space. [50] The masses of the first two generations of squarks $\tilde{d}_{iL}$ are essentially equal to their soft breaking masses, which receive renormalization effects only from gaugino loops, and hence degenerate. The soft breaking mass of $\tilde{b}_L$ is much smaller than that of the other two generations, as we will see, since the $\tilde{b}_L$ belongs to the same multiplet as the top above M_G. Noting that there is no mixing at the b_R-$\tilde{b}_R$-gaugino vertex introduced by SU(5) grand unification, and using the unitarity of the CKM matrix $\mathbf{V}$, one may express the contributions to A_γ by the gluinos [36–38,51] as follows:

$$\begin{aligned} A_\gamma^{\tilde{g}} &= C(R) e_D M_W^2 \frac{\alpha_s}{\alpha_2} \{ \frac{g_1\left(m_{\tilde{Q}_{3L}}\right) - g_1\left(m_{\tilde{Q}_{1L}}\right)}{M_3^2} \\ &+ \eta_b^{-1} \left(A_b + \mu \tan\beta\right) \left[G\left(m_{\tilde{b}_R}, m_{\tilde{Q}_{3L}}\right) - G\left(m_{\tilde{b}_R}, m_{\tilde{Q}_{1L}}\right) \right] \\ &+ \eta_b^{-1} \left(A_b - A_d\right) G\left(m_{\tilde{b}_R}, m_{\tilde{Q}_{3L}}\right) \} , \end{aligned} \tag{86}$$

where G is given by

$$G\left(m_1^2, m_2^2\right) = \frac{1}{M_3} \frac{g_2\left(\frac{m_1^2}{M_3^2}\right) - g_2\left(\frac{m_2^2}{M_3^2}\right)}{m_1^2 - m_2^2} , \tag{87}$$

with

$$g_1(r) = \frac{1}{6(r-1)^4} [2 + 3r - 6r^2 + r^3 + 6r \ln r] , \tag{88}$$

$$g_2(r) = \frac{-1}{2(r-1)^3}[r^2 - 1 - 2r\ln r], \tag{89}$$

where we have used $e_D = -1/3$, $C(R) = 4/3$, and $\eta_b \equiv m_b(m_b)/m_b(M_W)$, which we take to be $\eta_b = 1.5$. The analogous expression for neutralinos may be obtained from the above expressions by working in the neutralino mass eigenbasis and noting that the first term in Eq. (87) comes from the diagram of Fig. 10a with the bino propagator and the other terms come from Fig. 10b with the bino-wino propagator (See, for example, ref. [51].). We have not included the diagram with the higgsino-wino propagator. Because neutralinos do not interact with gluons, one finds that simply $A_g^{\tilde{\chi}^0} = A_\gamma^{\tilde{\chi}^0}/e_D$. On the other hand, because a gluon can attach to the gluino propagator, one finds

$$A_g^{\tilde{g}} = -\frac{C(G)}{C(R)}\frac{1}{2e_D}A_\gamma^{\tilde{g}}[g_1 \to h_1, g_2 \to h_2] + \frac{1}{2e_D}(2 - C(G)/C(R))A_\gamma^{\tilde{g}}, \tag{90}$$

with $C(G) = 3$ and

$$h_1(r) = (1 - 6r + 3r^2 + 2r^3 - 6r^2\ln r)/6(r-1)^4, \tag{91}$$

$$h_2(r) = -(-1 + 4r - 3r^2 + 2r^2\ln r)/2(r-1)^3. \tag{92}$$

Notice that the gluino contribution to $b \to g\gamma$ can be highly significant.

The mass of $\tilde{Q}_{3L}$ may be expressed in terms of the first generation squark mass $m^2_{\tilde{Q}_{1L}}$ as

$$m^2_{\tilde{Q}_3 L} = m^2_{\tilde{Q}_{1L}} - \left(I_G + \frac{I_Z}{2}\right), \tag{93}$$

where $I_G = (3/8\pi^2)\int_{M_G}^{M_P}\lambda_t^2\left(m_H^2 + 2m^2_{\mathbf{10}_3} + A_t^2\right)d\ln\mu$, and I_Z is the analogous contribution obtained from running the scale down from M_G to M_W. The integrals I_G and I_Z may be obtained from the analytic one loop solutions in terms of $m^2_{\tilde{Q}_{1L}}$ and $M_3(M_W)$ as follows:

$$I_G \approx 0.80 m^2_{\tilde{Q}_{1L}} - 0.71 M_3^2\,,\; I_Z \approx 0.19 m^2_{\tilde{Q}_{1L}} + 0.17 M_3^2\,, \tag{94}$$

where we have taken $M_P = 2.4\,10^{18}$GeV. One can also find that the relevant weak scale trilinear scale couplings are $A_b \approx -1.38 M_3$ and $A_d \approx -1.55 M_3$. We calculate the parameter μ at the tree level and find $\mu^2 \approx 1.0 m^2_{\tilde{Q}_{1L}} - 0.038 M_3^2 - 4200\text{GeV}^2$.

Comparison with the Experimental Result

To illustrate the relative sizes of the separate contributions to the $b \to s\gamma$ rate, we plot

$$r_{A_i} \equiv A^i/A^W \tag{95}$$

versus gluino mass for different values of $m_{\tilde{Q}_{1L}}$ in Fig.11 for the case $\mu > 0$, with

$$A^i \equiv \eta^{16/23}[A^i_\gamma - (8/3)A^i_g(1-\eta^{-2/23})]\,, \tag{96}$$

$$A^W \equiv \eta^{16/23}[A^W_\gamma - (8/3)A^W_g(1-\eta^{-2/23})] + \sum_{i=1}^{8} a_i\eta^{b_i}\,. \tag{97}$$

Notice that the gluino contribution to A_γ is sometimes even bigger than that of the chargino. This happens when the gluino mass is light. In Fig. 2c, for the gluino contribution, we also plot dashed lines which correspond to the approximation $c_8(M_W) = 0$, i.e. the approximation $A^{\tilde{g}}_g = A^W_g = 0$. It should be noticed that including the O_8 operator in the running of c_7 below the scale M_W can lead to the gluino contribution being as much as 50-percent more important for a light gluino mass. Note that the neutralino contribution is insignificant as usual. In fact, unlike with the gluino contribution, including $A^{\tilde{\chi}^0}_g$ in $c_7(M_W)$ decreases the neutralino contribution to the decay. In Fig. 12, we plot the resulting branching ratio for $b \to s\gamma$. The dotted line corresponds to the calculation neglecting gluino and neutralino mediated contributions, while the solid line represents the full calulation. In both cases, we have included the SM, charged Higgs and chargino corrections as found in [39], which work very well for low $\tan\beta$. When the glunino mass is 150 GeV, the gluino contribution can increase the branching ratio by as much as about 20-percent. In Fig. 13 and 14, we depict the analogous situation with the universal boundary condition taken at the GUT scale. Notice that when gluino masses are light, the gluino contributions are about one-third the size as when the boundary condition is taken at the Planck scale. The effect of taking the universal boundary condition at the Planck scale has only a small effect on the total chargino contribution for the parameter space shown here. However, we find that for other nearby regions, for example with $\tan\beta = 2$, the

effect of making the chargino contribution more positive, but smaller in magnitude, is more apparant. In Fig. 15a and 15b, we plot the branching ratio as a function of the M_G scale gaugino mass M_{5G} for curves of constant m_0 for the cases where the universal boundary condition is taken at the Planck scale and at the scale M_G, respectively. Notice that for the curves with $m_0 > 0$, the branching ratios for the complete calculation in the two cases differ by about 10-percent when M_{5G} =60 GeV. The latter corresponds to a not very light gluino mass of about 170 GeV. When $\mu < 0$ and $\tan\beta$ is of order 1, we find the contribution to be much less important due to a strong destructive interference between the two diagrams in Fig. 10.

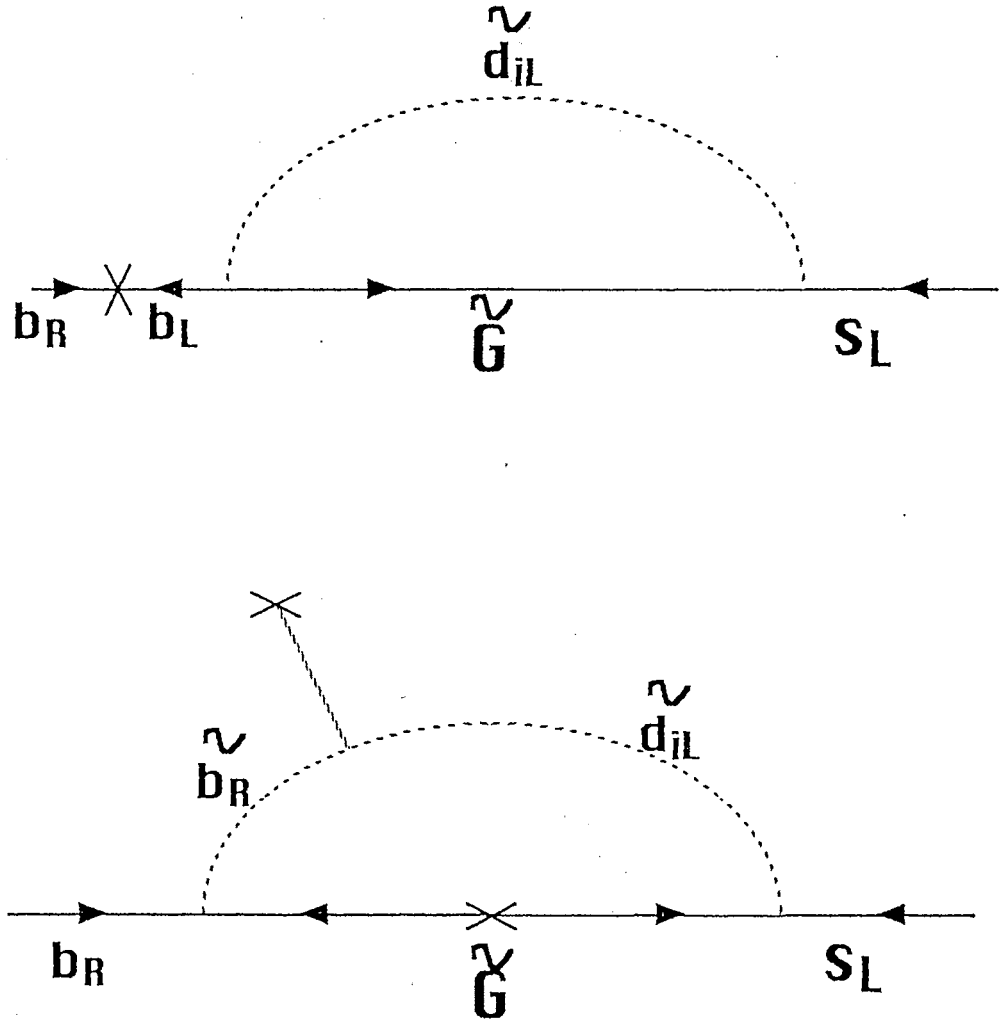

Figure 10. The two types of diagrams with $\tilde{d}_{iL}$ running in the internal loop that can contribute signifigantly to $b_R \to s_L\gamma$ and $b_R \to s_L g$. One must sum the graphs with an external photon or gluon attached in all possible ways.

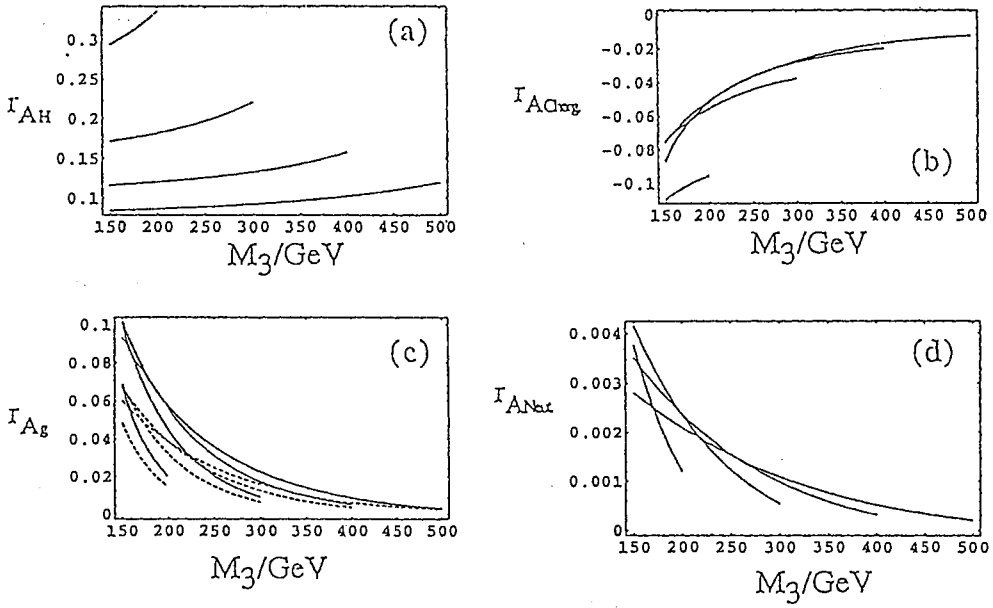

Figure 11. Plots of $r_{A_i} \equiv A^i/A^W$, which includes QCD corrections, versus gluino mass for different values of $m_{\tilde{Q}_{1L}}$ for the case $\mu > 0$ and $\tan\beta = 1.5$ with the universal boundary condition taken at the scale M_P. In Fig. c for $r_{A_{\tilde{g}}}$, the dashed lines represent the approximation $c_8(M_W) = 0$. The curves correspond to squark masses $m_{\tilde{d}_L}$ =200, 300, 400, and 500 GeV. The gluino masses for each curve range from 150 GeV to the corresponding value of $m_{\tilde{d}_L}$. For example, $m_{\tilde{d}_L}$ =200 GeV corresponds to the curve for which the gluino mass ranges from 120 Gev to 200 GeV. Figs.a, b , c, and d correspond to the charged Higgs, chargino, gluino, and neutralino contributions, respectively.

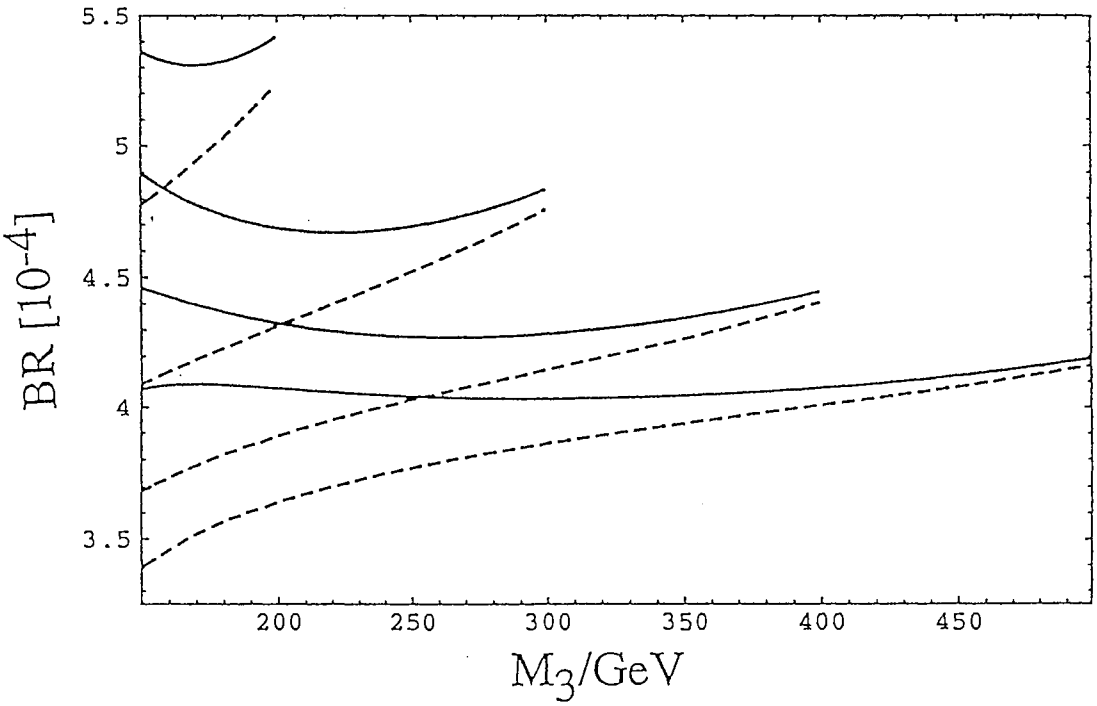

Figure 12. Plots of the branching ratio of $b \to s\gamma$ for the case of Fig. 11. The solid lines represent the calculation including SM, charged Higgs, chargino, gluino, and neutralino contributions. The dashed lines represent the calculation using only the SM, charged Higgs, and chargino contributions. The curves represent the same squark masses as have been used in Fig. 11.

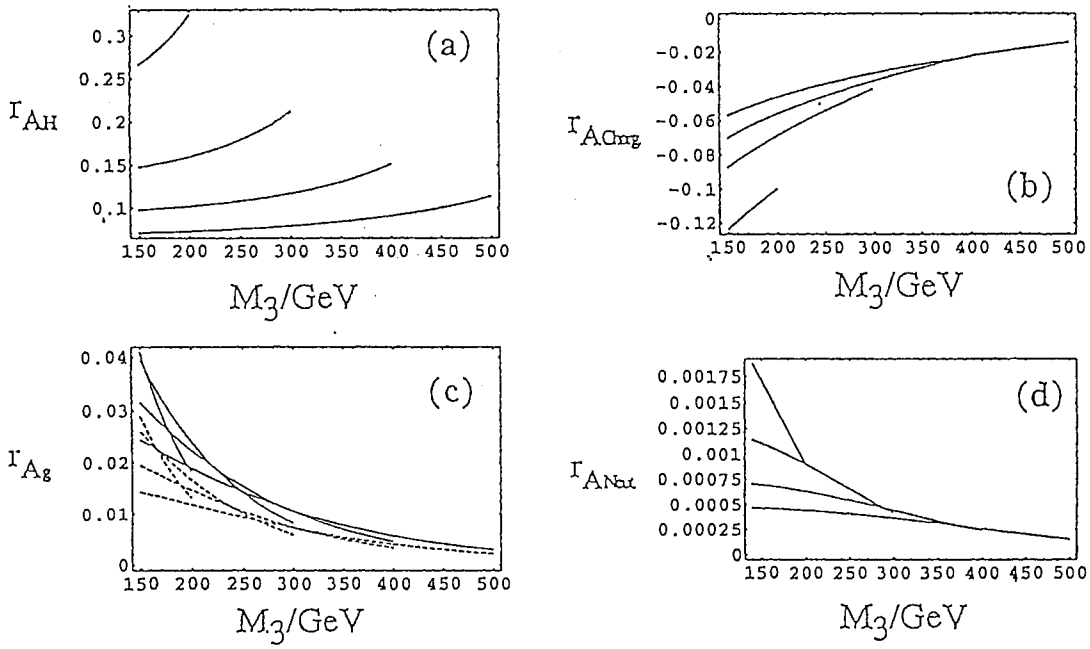

Figure 13. Same as Fig. 11, but with the universal boudary condition taken at the M_G scale.

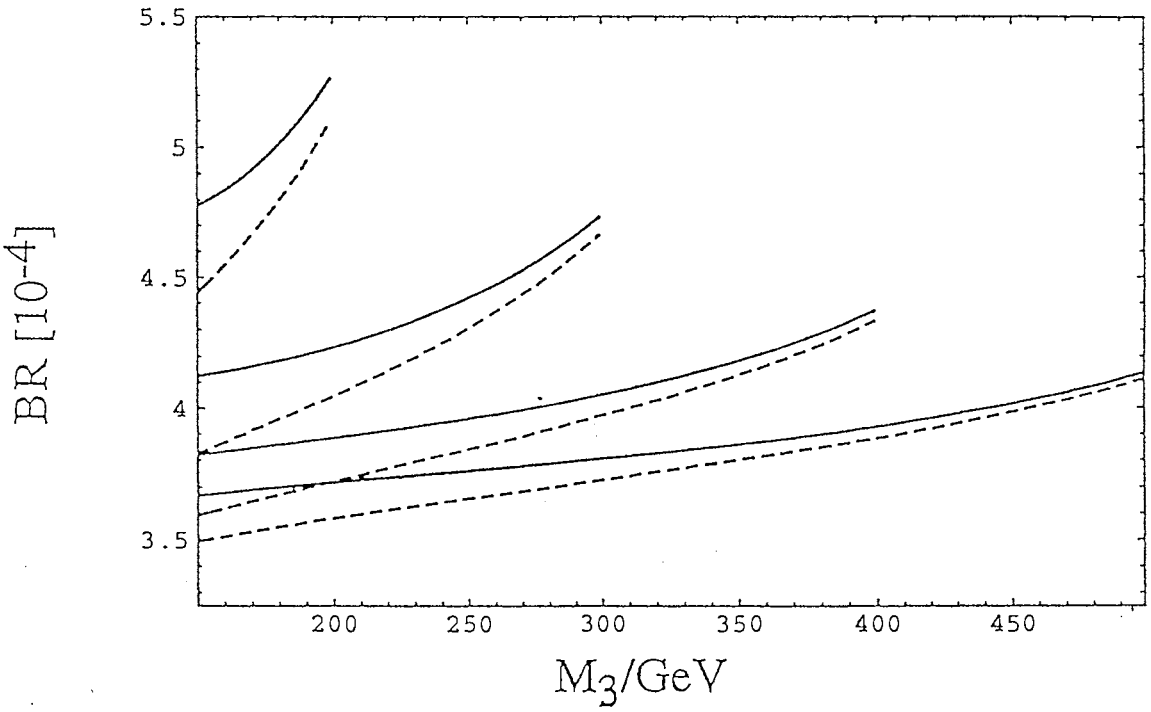

Figure 14. Same as Fig. 12, but with the universal boudary condition taken at the M_G scale.

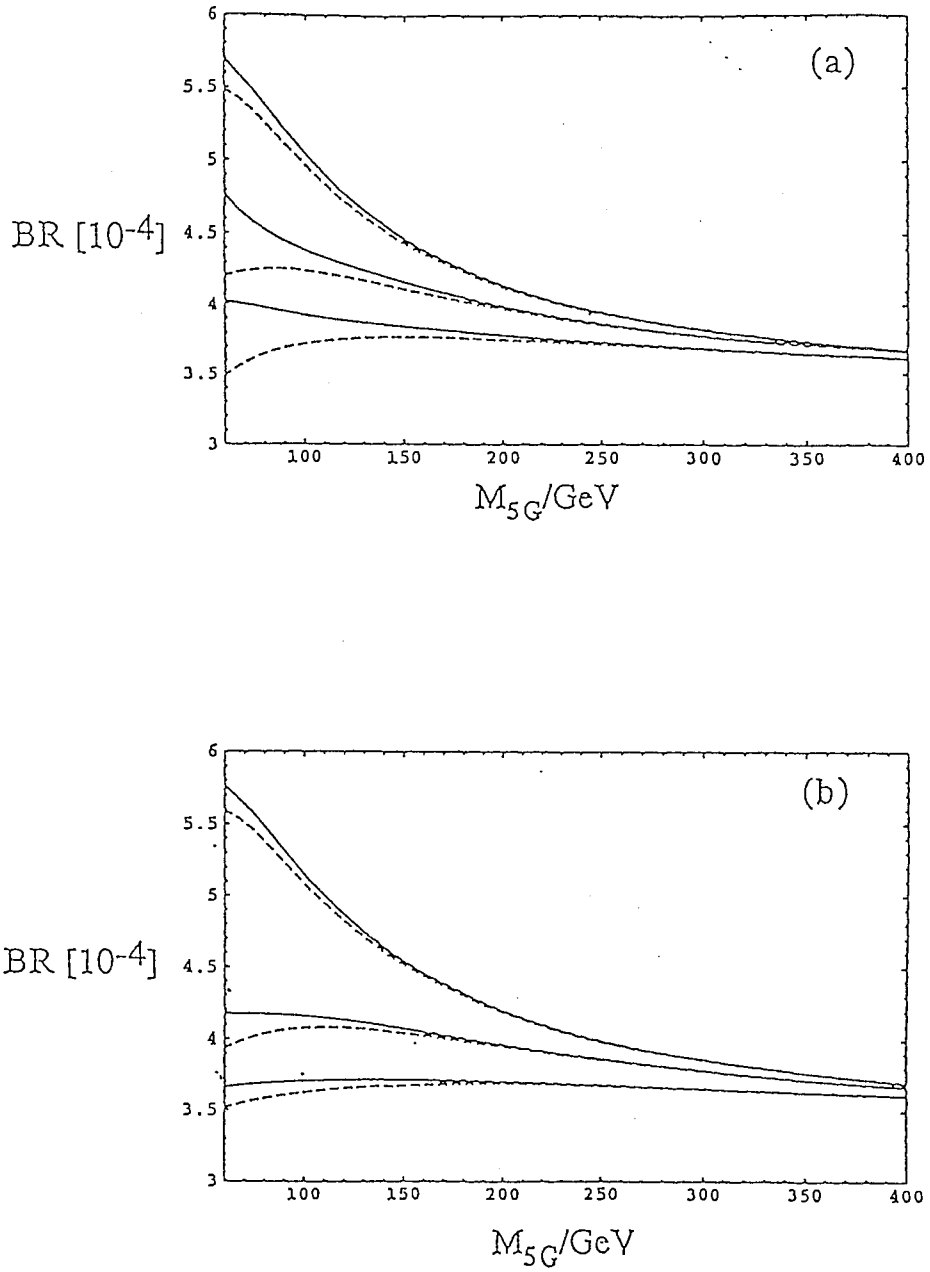

Figure 15. Plots of the branching ratio for the case of $\mu > 0$ and $\tan\beta = 1.5$ as a function of the M_G scale gaugino mass M_{5G} for curves of constant m_0. fig.a corresponds to the universal boundary condition taken at the Planck scale. fig.b corresponds to the universal boundary condition taken at the GUT breaking scale. The solid lines represent the calculation including SM, charged Higgs, chargino, gluino, and neutralino contributions. The dashed lines represent the calculation using only the SM, charged Higgs, and chargino contributions. The curves represent, in descending order in the two plots, m_0 =0, 250 GeV, and 500 GeV.

CHAPTER V

CONCLUSION

Here let us summarize the main points discussed in the previous chapters.

First, let us summarize our main results for the extra Z . In the class of models in which the extra Z boson does not directly couple to the fermions, the best way to produce and observe it in the hadronic supercolliders is via the resonant process . The cross- sections are fairly large to be observable, but they are very sharply peaked around the Z_2 mass. Thus, the final state pair will also have a sharp peak in the energy distribution of the pairs. If the detector energy resolution is very broad, the signal will still be observable as the excess of pairs in the integrated cross-section. If both a Higgs boson and an extra Z boson are present with roughly the same mass, (say in the range 800 GeV to 1.5 TeV), detailed study of the angular distribution of the pair could disentangle the two signals.

Now the major results for the dileptons. Doubly charged dilepton gauge bosons (Y^{++}) can be copiously produced at the LHC. The associated multilepton events will have peaks in the invariant mass distribution of the same sign dilepton pairs, thereby easily distinguishing them from the usual standard model backgrounds. At LHC, a dilepton gauge boson mass, $M_{Y_{++}}$ (up to 1.5 TeV or less) can be explored. Current Fermilab Tevatron experiments should see such events or set a lower bound on $M_{Y_{++}}$ of about 200 GeV, while future upgrade could push the bound to about 400 GeV.

For the extension of color sector let us summarize our main points. At Fermilab energies, we have calculated the branching ratios for the various final states possible from a $t\bar{t}$ pair produced through resonant coloron. This is quite model dependent; however, the motivation for these model is that they can give a larger cross section than the SM. Thus we choose sets of parameters which give a production cross section of about three times the SM cross section. Our results are shown in Table III and IV.

We see that the branching ratios for the interesting final states are not very different from those of the standard model unless we take a large value for the minimum p_T. This seems to be in agreement with Ref. [10]. We have chosen to require a large transverse momentum for the jets and leptons because it was hoped that these models would be distinguished by larger branching ratios for large transverse momentum.

The only check we have on the accuracy of the numbers in any of the tables is to rerun the Monte Carlo integral which generates the histograms with different sets of random numbers. When we do this the branching ratios, even those whose values are very small, remain very stable; nevertheless we feel the very small numbers should not be trusted.

At LHC energies we have calculated the branching ratios for the various final states of coloron-coloron$\rightarrow t\bar{t}\ t\bar{t}$ production. These are given in Tables V, VI and VII. Here we have many final states that are only possible in higher order in the SM; if n is the number of jets and m is the number of electron or muons these final states are $m > 2$ if $n \leq 2$, $m > 1$ if $3 \leq n \leq 4, m > 0$ if $5 \leq n \leq 6$. Even when the branching ratios for these states are rather small, this is compensated by a large production cross section if the coloron mass is not too large. Detection of these states would be a very strong signal for the coloron.

For $b- > s\gamma$, if one is to calculate the decay rate for the flavor changing process $b \rightarrow s\gamma$ in a SUSY GUT with SUSY breaking communicated by gravity above the GUT breaking scale in the form of soft breaking mass terms, it is essential to include the GUT scale renormalization group effects. An important result of including these renormalization effects is that the gluino contribution to the decay rate can now no longer be neglected when the glunino mass is relatively light.

So we observe the available experimental data actually support lots of theories beyond the Standard Model. though it does not pick any one particular. This nonuniqueness would be hopefully resolved in the near future when LHC starts working. Probably then we will be able to explain everything from Planck scale down to weak scale by one complete theory.

BIBLIOGRAPHY

1. S. L. Glashow, Nucl. Phys. Rev. **22,** 579 (1961). S. Weinberg, Phys. Rev. Lett. **19** ,1264 (1967). A. Salam, *In Elementary Particle physics*: Nobel Symp. No. 8, ed. N. Svartholm. Stockholm. Stockholm, 1968.

2. C. N. Yang and R. L. Mills, Phys. Rev. **96**, 191 (1954). M. Gell-mann and S.L.Glashow, Ann.Phys.(NY) **15**, 437 (1961).

3. G.'t Hooft, Nucl. Phys. **B33** , 173 (1971). G.'t Hooft, Nucl. Phys. **B35** , 167 (1971).

4. Y. Nambu, Phys. Rev. Lett. **4** , 380 (1960). P. W. Higgs, Phys. Rev. Lett. **13** , 508 (1964). T. W. B. Kibble, Phys. Rev. **155**, 1554 (1967).

5. N. cabbibo, Phys. Rev. Lett. **10** , 531 (1963). M. Kobayashi and T. Maskawa, Prog. Theor. Phys. **49**,652 (1973).

6. D. Volkov and V. P. Akulov, JETP Lett. 16, 438 (1972). J. Wess and B. Zumino, Nucl. Phys. **B70,** 39 (1974). J. Wess and B. Zumino, Phys. Lett. **B49,** 52 (1974).

7. H. E. Haber and G. L. Kane, Phys. Rep. **117**, 75 (1985), and references therein.

8. D. London and J. L. Rosner, Phys. Rev. **D34**, 1530 (1986).

9. P. H. frampton, Phys. Rev. Lett. **69** (1992) 288.

10. C. T. Hill, S. J. Parke, Phys. Rev. **D49** 4454 (1994); C.T. Hill, Phys. Lett. . 419 (1991).

11. For example, see J. L. Hewett and T. G. Rizzo, Phys. Rep. **183** (1989) 195.

12. E. Nardi, E. Roulet and D. Tommasini, Phys. Rev. **D 46** (1992) 3040.

13. P. Langacker and M. Luo, Phys. Rev. **D 45** (1992)278.

14. P.Langacker, M. Luo and A. K. Mann, Rev. Mod. Phys. **64** (1992) 87.

15. M. Cvetic and P. Langacker, Univ. of Pensylvania report UPR-533-T, Talk presented at the XXVI International Conference on High Energy Physics, Aug. 6-12, 1992 at Dallas Texas, August 1992).

16. K. T. Mahanthappa and P. K. Mohapatra, Phys. Rev. **D 43** (1991) 3093.

17. B. Dutta and S. Nandi, Phys. Lett. **B,** 315 (1993) 134.

18. S. Nandi, Phys. Lett. **B 188** (1987) 159. S. Nandi and T. G. Rizzo, Phys. Rev. **D 37** (1988) 52.

19. N. G. Deshpande, K. Panose and J. Trampetic, Phys. Lett **B 214** (1988) 467.

20. V. Barger and K. Whisnant, Int. J. Mod. Phys. **A3** (1988) 897. S. Nandi, Phys. Lett. **B 181** (1986) 375; T. G. Rizzo, Phys. Rev. **D 34** (1986) 1438, R. W. Robinett, Phys. Rev. **D 34** (1986) 182.

21. F. Pisano and V. Pleitez, Phys. Rev. D **46** (1992) 10.

22. Jogesh C. Pati,; A. Salam and J. Strathdee, Phys. Lett. **108B** (1982) 121.

23. P. H. Frampton and B. H. Lee, Phys. Rev. Lett. **5.**

24. P. H. Frampton, Mod. Phys. Lett. **A 7** (1992) 559.

25. B. Dutta and S. Nandi, Phys. Lett. **B** 340 (1994) 86.

26. E. Eichten, I. Hinchcliffe, K. Lane and C. Quigg, Phys. Rev. D **34** (1986) 1547.

27. B. Bailey, J. F. Owens and J. Ohnemus, Phys. Rev. **D46**, (1992) 2018; J. F. Gunion, G. L. Kane and Jose Wudka, Nucl. Phys. **B299** (1988) 291.

28. F. Abe et. al, Phys. Rev. Lett. **73,** 225(1994); ibid, Phys. Rev. D 50, 2966 (1994).

29. E. Laenen, J. Smith, and W. L.Van Neerven, Phys. Lett. **B321,** 254(1994).

30. E. Eichten and K. Lane. FERMILAB-PUB-94/007-T/BUHEP-94-1(1994); T.Appelquist and G.Triantaphyllou, Phys. Rev. Lett. **69,** 2750 (1992); E. Eichten, I. Hinchcliffe, K. Lane and C. Quigg, Phys. Rev. **D 34**, 1547 (1986).

31. V. Barger and R.J.N. Phillips. University of Wisconsin Preprint, MAD/PH/830 (1994), hep-ph 9405224; W. S. Hou and H. Huang, National Taiwan University Preprint, NTUTH-94-18(1994) (hep-ph 9409227); W. S. Hou, Phys. Rev. Lett. 72, 3945 (1994); B. Mukhopadhyaya and S. Nandi, Phys. Rev. Lett. **66**, 285 (1991); ibid; Phys. Rev.**D.46**, 5098 (1992); T. P. Cheng and L. -F. Li, Phys. Rev **D45**, 1708 (1992) W. S. Hou, Phys. Rev. Lett. 69, 3587(1992); B. Mukhopadhyaya and S. Nandi, Phys. Rev. Lett. **24**, 3588 (1992).

32. D. Atwood, A. Kagan and T.G. Rizzo, SLAC-PUB-6580, July, 1994; G. L. Kane, G. A. Ladinsky and C. P. Yuan, Phys. Rev. **D** 45, 124 (1992).

33. B. Dutta and S. Nandi, Phys. Rev. **D** (to be published)

34. M. Lindner and D. Ross, Nucl. Phys. **B** 370, 30 (1992).

35. R. Brock et. al. (CTEQ Collaboration), "Handbook of Perturbative QCD, Version 1.0", Fermilab-Pub-93-094 (1993).

36. S. Bertolini, F. Borzumati, and A. Masiero, Nucl. Phys. B294, 321 (1987).

37. S. Bertolini, F. Borzumati, A. Masiero, and G. Ridolfi, Nucl. Phys. B353, 591 (1991).

38. N. Oshimo, Nucl. Phys. B404, 20 (1993).

39. R. Barbieri and G. F. Giuidice, Phys. Lett. B309, 86(1993)

40. V. Barger, M. Berger, P. Ohmann, and R. J. N. Phillips, Phys. Rev. D51, 2438 (1995), and references therein.

41. R. Arnowitt and Pran Nath, CTP-TAMU-65/94, NUB-TH-3111/94.

42. J. L. Hewett, SLAC-PUB-6521.

43. M. A. Diaz, Phys. Lett. B322, 207 (1994).

44. R. Garisto and J. N. Ng, Phys. Lett. B315, 372 (1993).

45. F.Borzumati, Z. Phys. C63, 291 (1994).

46. J. L. Lopez, D. V. Nanopoulos, and K. Yuan, Phys. Lett. B267, 219 (1991); S. Kelly, J. L. Lopez, D. V. Nanopoulos, H. Pois, and K. Yuan, Phys. Rev. D47, 2461 (1993).

47. S. Bertolini and F. Vissani, SISSA 40/94/EP.

48. N. Polonsky and A. Pomarol, Phys. Rev. Lett. 73, 2292 (1994); N. Polonsky and A. Pomarol, UPR-0627T.

49. R. Barbieri and L. J. Hall, Phys. Lett.B338 212, (1994).

50. S. Dimopolous and L. J. Hall, LBL-36269, UCB-PTH-94/25.

51. R. Barbieri, L. J. Hall, and A. Strumia, LBL-36381, IFUP-TH 72/94, UCB-PTH-94/29.

52. L. J. Hall, V. A. Kostelecky, and S. Raby, Nucl. Phys.B267 415, (1986).

53. T. Inami and C. S. Lim, Prog. Theor. Phys 65, 297 (1981).

54. N. G. Deshpande and G. Eilam, Phys. Rev. D26, 2463 (1982)

55. M. Misiak, Phys. Lett. B269, 161 (1991).

56. A. J. Buras, M. Misiak, M. Munz, and S. Pokorski,Nucl. Phys. B424, 374 (1994).

57. V. Barger, M. Berger, and P. Ohmann, Phys. Rev.D49 4908 (1994).

58. B. Dutta and E. Keith, OSU Preprint 298

59. K. Inoue, A. Kakuto, H. Komatsu, and S. Takeshita, Prog. Theo. Phys. 68 927 (1982).

60. B. Dutta, E. Keith, and T. V. Duong, (in preparation).

VITA

BHASKAR DUTTA

Candidate for the Degree of

Doctor of Philosophy

Thesis: BEYOND THE STANDARD MODEL

Major Field: Physics

Biographical:

Personal Data: Born in City of Calcutta, West Bengal, India, August 12, 1965, the son of Mr. Shyamal Kr. Dutta and Mrs. Jharna Dutta.

Education: Graduated from Ballygunge Government High School, Calcutta, India, in July, 1984; received Bachelor of Science Degree in Physics from Presidency College (Calcutta University), Calcutta, India, in December, 1987; received Masters of Science Degree from Calcutta-University, Calcutta, India, in July, 1990; completed the requirements for the Doctor of Philosophy Degree at Oklahoma State University in July, 1995.

Professional Experience: Research and Teaching Assistant, Department of Physics, Oklahoma State University, August, 1990 to July, 1995.